Knockout of the Hmt1p Arginine Methyltransferase in *Saccharomyces cerevisiae* Leads to the Dysregulation of Phosphate-associated Genes and Processes

Authors

Samantha Z. Chia, Yu-Wen Lai, Daniel Yagoub, Sophie Lev, Joshua J. Hamey, Chi Nam Ignatius Pang, Desmarini Desmarini, Zhiliang Chen, Julianne T. Djordjevic, Melissa A. Erce, Gene Hart-Smith, and Marc R. Wilkins

Correspondence

m.wilkins@unsw.edu.au

In Brief

Arginine methylation of proteins in the eukaryotic cell is predominantly catalyzed by one conserved enzyme; PRMT1 in mammals or Hmt1p in yeast. Knockout in mammals is embryonic lethal; however, Hmt1p in yeast is non-essential. The systems-level effects of *hmt1* knockout in yeast were investigated. Unexpected but significant dysregulation in phosphate homeostasis was seen upon *hmt1* knockout. Transcription factor-driven processes may explain these observations, or regulatory processes may link the sensing of *S*-adenosylmethionine to intracellular phosphate or polyphosphate.

Graphical Abstract

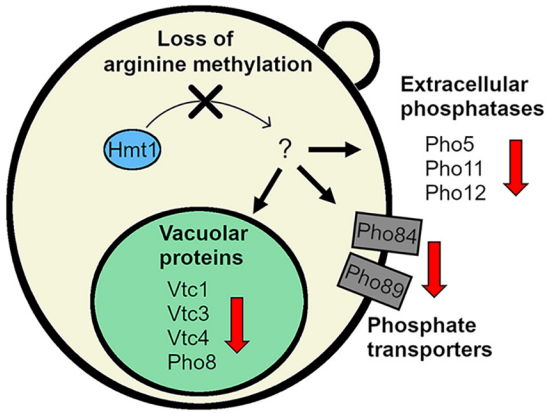

Highlights

- Knockout of arginine methyltransferase Hmt1p in *S. cerevisiae* was investigated.
- RNA-seq and SILAC MS/MS found downregulation of phosphate-associated processes.
- Phosphate homeostasis and extracellular levels of acid phosphatases were perturbed.
- Pho4p was an *in vitro* Hmt1p substrate, but this was not confirmed *in vivo*.

Chia et al., 2018, Molecular & Cellular Proteomics *17*, 2462–2479

https://doi.org/10.1074/mcp.RA117.000214

Knockout of the Hmt1p Arginine Methyltransferase in *Saccharomyces cerevisiae* Leads to the Dysregulation of Phosphate-associated Genes and Processes*[S]

Samantha Z. Chia‡‖, Yu-Wen Lai‡‖, Daniel Yagoub‡‖, Sophie Lev§, Joshua J. Hamey‡, Chi Nam Ignatius Pang‡, Desmarini Desmarini§, Zhiliang Chen‡, Julianne T. Djordjevic§, Melissa A. Erce‡, Gene Hart-Smith‡, and Marc R. Wilkins‡¶

Hmt1p is the predominant arginine methyltransferase in *Saccharomyces cerevisiae*. Its substrate proteins are involved in transcription, transcriptional regulation, nucleocytoplasmic transport and RNA splicing. Hmt1p-catalyzed methylation can also modulate protein-protein interactions. Hmt1p is conserved from unicellular eukaryotes through to mammals where its ortholog, PRMT1, is lethal upon knockout. In yeast, however, the effect of knockout on the transcriptome and proteome has not been described. Transcriptome analysis revealed downregulation of phosphate-responsive genes in *hmt1*Δ, including acid phosphatases *PHO5*, *PHO11,* and *PHO12*, phosphate transporters *PHO84* and *PHO89* and the vacuolar transporter chaperone *VTC3*. Analysis of the *hmt1*Δ proteome revealed decreased abundance of phosphate-associated proteins including phosphate transporter Pho84p, vacuolar alkaline phosphatase Pho8p, acid phosphatase Pho3p and subunits of the vacuolar transporter chaperone complex Vtc1p, Vtc3p and Vtc4p. Consistent with this, phosphate homeostasis was dysregulated in *hmt1*Δ cells, showing decreased extracellular phosphatase levels and decreased total P_i in phosphate-depleted medium. *In vitro*, we showed that transcription factor Pho4p can be methylated at Arg-241, which could explain phosphate dysregulation in *hmt1*Δ if interplay exists with phosphorylation at Ser-242 or Ser-243, or if Arg-241 methylation affects the capacity of Pho4p to homodimerize or interact with Pho2p. However, the Arg-241 methylation site was not validated *in vivo* and the localization of a Pho4p-GFP fusion in *hmt1*Δ was not different from wild type. To our knowledge, this is the first study to reveal an association between Hmt1p and phosphate homeostasis and one which suggests a regulatory link between S-adenosyl methionine and intracellular phosphate. *Molecular & Cellular Proteomics 17: 2462–2479, 2018. DOI: 10.1074/mcp.RA117.000214.*

Hmt1p is the predominant arginine methyltransferase in yeast (1). It has an abundance of ~37,600 copies per cell and is responsible for 66% of arginine monomethylation and 89% of asymmetric dimethylation of intracellular proteins (2, 3). Its substrates, identified through a series of proteome-scale and targeted approaches (4–7), include both histone and non-histone proteins. In the case of histone proteins, Hmt1p asymmetrically dimethylates histone H4 on Arg-3 (H4R3me2a) and contributes to the histone code through gene silencing (8, 9). On non-histone proteins, Hmt1p-mediated mono- and asymmetric di-methylation of arginine is implicated in transcriptional regulation, nucleocytoplasmic shuttling of proteins and mRNA, and to a lesser extent RNA processing and translational regulation (reviewed in (10)). In total, Hmt1p has been shown to have at least 25 substrate proteins, 10 of which have been validated *in vitro* (10, 11).

Hmt1p is conserved across model eukaryotes (such as *Arabidopsis thaliana*, *Drosophila melanogaster*, *Caenorhabditis elegans*) (12). In mammals, the predominant mammalian arginine methyltransferase, PRMT1, is the ortholog of Hmt1p and is involved in functions including genome integrity, cell proliferation and response to DNA damage (13). Interestingly, the dysregulation of PRMT1 is associated with human diseases such as cardiovascular disease and cancer (14) and in mice, knockout of PRMT1 is embryonic lethal (15). Despite arginine methylation being implicated in a plethora of biological processes, *HMT1* in *S. cerevisiae* is not essential. The knockout has not been documented to show a clear metabolic phenotype (16), but has been reported to show increased transcription from silent chromatin regions because of loss of H4R3me2a (17) and higher tRNA abundance compared with the wild-type (18).

From the ‡Systems Biology Initiative, School of Biotechnology and Biomolecular Sciences, University of New South Wales, Sydney, NSW 2052, Australia; §Centre for Infectious Diseases and Microbiology, Westmead Millennium Institute and Sydney Medical School, University of Sydney at Westmead Hospital, Westmead, New South Wales, Australia

Received July 26, 2017, and in revised form, August 14, 2018
Published, MCP Papers in Press, September 11, 2018, DOI 10.1074/mcp.RA117.000214

Phosphate is a critical macronutrient that is required for energy generation via ATP and GTP synthesis and DNA, RNA and phospholipid biosynthesis. It is also important for cellular signaling processes via phosphor transfer reactions that affect protein function and activity. In yeast, the phosphate (PHO)[1] pathway is modulated by phosphate availability in the environment and the phosphate requirements within the cell. The PHO pathway is regulated by the transcription factor Pho4p and its target genes involve those that encode for membrane-embedded phosphate transporters *PHO84*, *PHO89*, *PHO87*, *PHO90*, *PHO91,* acid phosphatases *PHO5*, *PHO11* and *PHO12*, and polyphosphate synthetases and transporters *VTC1*, *VTC2*, *VTC3*, and *VTC4* (19, 20). Under phosphate limitation Pho4p becomes activated and transcribes extracellular phosphatases and transporters that sequester extracellular inorganic phosphate (P_i) from phosphate containing organic compounds and imports this P_i into the cell (19). Within the cell, excess cytosolic P_i is usually synthesized into polymers of P_i known as polyphosphates (polyP) and transported through the vacuole membrane for storage by the multi-subunit vacuolar transporter chaperone (VTC) complex (19, 21, 22). polyP acts as an internal P_i buffer and is mobilized from the vacuole and converted into single P_i under phosphate limitation (23). polyP has been shown to serve other functions in the cell, with implications in cell cycle progression, metal chelation, pathogenicity, cellular stress and survival (24–26).

To discover novel functions of Hmt1p, here we first investigated the changes in the transcriptome and proteome in the *HMT1* deletion mutant, which revealed an apparent dysregulation in phosphate homeostasis. In *hmt1*Δ, many components of the PHO pathway, including repressible acid phosphatases, phosphate transporters and vacuolar transporter chaperone proteins showed downregulation and/or lower abundance in *hmt1*Δ as compared with wild-type yeast during mid-log growth. These results were associated with a decrease in phosphatase production, a decrease in total P_i in phosphate depleted medium, and the dysregulation of polyP homeostasis within the *hmt1*Δ cell. We further showed that the transcription factor Pho4p can be methylated, at Arg-241, by *in vitro* incubation with Hmt1p. Our study is the first to establish an association between Hmt1p-mediated arginine methylation, the regulation of the PHO pathway and of phosphate metabolism.

[1] The abbreviations used are: PHO, phosphate/phosphate responsive signaling pathway; P_i, inorganic phosphate; polyP, polyphosphates; VTC, Vacuolar Transporter Chaperone; SILAC, stable isotope labelling with amino acids in cell culture; pNPP, *p*-nitrophenyl phosphate; ScPpx1p, exopolyphosphatase of *S. cerevisiae*; MM-KCl, low phosphate medium; MM-KH2PO4, high phosphate medium; YEPD, Yeast extract peptone dextrose; LB, Luria broth; BWA, Burrows-Wheeler Aligner; HTSeq, High Throughput Sequencing; IPTG, isopropyl β-D-1-thiogalactopyranoside; SAM, S-Adenosyl methionine; ETD, electron transfer dissociation; R241, Arg-241; SLIM, site-directed ligase independent mutagenesis; SC-URA, synthetic complete medium with uracil drop-out; FITC, fluorescein isothiocyanate; GFP, green fluorescent protein; DAPI, 4′,6-diamidino-2-phenylindole; PRIDE, PRoteomics IDEntifications; SRA, sequence read archive; GO, gene ontology; CC, cellular compartment; BP, biological process; MF, molecular function; MMA, monomethylamine; MMG, monomethylguanidine; bHLH, basic helix–loop–helix; hnRNP, heterogeneous nuclear ribonucleoproteins; O-GlcNAc, O-linked β-N-acetyl glucosamine; KATs, lysine acetyltransferases.

EXPERIMENTAL PROCEDURES

Yeast Strains and Growth Conditions—*Saccharomyces cerevisiae* BY4741 haploid strain (Open Biosystems, Huntsville, AL; *MATa his3Δ1 leu2Δ0 met15Δ0 ura3Δ0*) was used as the wild-type in all experiments in this study unless otherwise specified. *HMT1* knockout yeast (Open Biosystems; *hmt1:: KANMX4* in BY4741) was used for studies related to deletion of arginine methyltransferase Hmt1p unless otherwise specified. Cells were maintained, and selection performed according to previous methods (27).

Strains were grown in YEPD (2% (w/v) D-glucose, 2% (w/v) bacteriological peptone, 1% (w/v) yeast extract), phosphate replete minimal media (MM-KH_2PO_4; 0.5% (w/v) KH_2PO_4, 15 mM D-glucose, 10 mM $MgSO_4.7H_2O$, 13 mM glycine, 3 μM thiamine) or phosphate depleted minimal media (MM-KCl; 0.5% (w/v) KCl, 15 mM D-glucose, 10 mM $MgSO_4.7H_2O$, 13 mM glycine, 3 μM thiamine) as specified.

For SILAC experiments, a BY4741 *lys2Δ/arg4Δ* strain was used where genes in the lysine and arginine biosynthetic pathways had been knocked out. This strain served as the background strain. *HMT1* was deleted from the BY4741 *lys2Δ/arg4Δ* strain by use of a hygromycin B resistance cassette amplified from plasmid pFA6a-hphNT1 as described in (28), resulting in *lys2Δ/arg4Δ/hmt1Δ* strain. Yeast cells were grown in synthetic complete media (2% (w/v) D-glucose, 0.5% (w/v) ammonium sulfate, 0.17% (w/v) yeast nitrogen base without amino acids or ammonium sulfate (BD Biosciences, San Jose, CA), with either 0.002% (w/v) "heavy" lysine-8 (13C615N2-L-lysine HCl, Munich, Germany) and arginine-10 (13C615N4-L-arginine HCl) (Silantes GmbH, Germany) or 0.002% (w/v) "light" L-lysine and L-arginine) at 30 °C with orbital shaking at 200 rpm.

Pho2p-GFP and Tef1p-GFP strains (*MATa his3Δ1 leu2Δ0 met15Δ0 ura3Δ0*) were acquired from Life Technologies (Carlsbad, CA). *HMT1* was deleted from Pho2p-GFP by use of a hygromycin B resistance cassette amplified from plasmid pFA6a-hphNT1 as described in (28). Pho4p-GFP (*pho4::PHO4-GFP ADE2* from K699 wild-type (*MAT***a** *ade2–1 trp1–1 can1–100 leu2–3,112 his3–11,15 ura3*)) was a gift from Erin O'Shea (Harvard) (29) and *HMT1* was deleted from this strain using a nourseothricin resistance cassette amplified from pFA6a-natNT2 (28).

Gene Expression Analysis and Raw Reads Filtering—Gene expression analysis was performed on three biological replicates each of wild-type and *hmt1*Δ, sampled at mid-logarithmic growth phase ($O.D._{600}$ = 0.8–1.0). Total RNA was extracted using TRIzol (Invitrogen, Carlsbad, CA) according to manufacturer's instructions. Ribosomal RNA depletion was performed prior to library generation (Ribominus Eukaryote kit, Life Technologies). The cDNA libraries for HiSeq 2000 sequencing were constructed from 10 μg of total RNA using the TruSeq SBS Kit v3-HS (Illumina, San Diego, CA) according to the manufacturer's instructions, generating 101 bp paired-end reads from a 160 bp insert library. RNA-Seq sequencing was performed using a HiSeq 2000 (Illumina), in the Ramaciotti Centre for Genomics, the University of New South Wales. Initial quality assessment for Illumina HiSeq sequence data was based on FastQC (version 0.11.2) (http://www.bioinformatics.babraham.ac.uk/projects/fastqc/). Pair-end raw reads were trimmed with the BWA trimming mode at a threshold of Q13 (p = 0.05) as implemented by SolexaQA version

1.11 (30). Low quality 3′-ends of each read were filtered. Reads that were less than 25 bp in length were discarded.

Mapping of RNA-Seq Reads and Differential Expression Analysis—Filtered reads from six samples were aligned to the *S. cerevisiae* S288C reference genome (version R64–1-1) (31) with TopHat 2.0.4 (32) and Bowtie 2–2.0.0-beta7 (33) using default parameters. Count files of the aligned sequencing reads were generated by the HTSeq-count script from the Python package HTSeq (34) with intersection-nonempty mode, using the GFF annotation file downloaded from the Saccharomyces Genome Database (35). Differential gene expression analysis was performed on the count files using the DESeq package (36) from Bioconductor (37), following standard normalization procedures. Genes with less than ten read counts in each replicate in both wild-type and *hmt1*Δ were removed from further analysis. Only genes differentially expressed at a false discovery rate ≤ 0.1 and adjusted p value < 0.05 were considered as significantly differentially expressed genes in the analysis.

Microarray Analysis—Total RNA was extracted from four wild-type and three *hmt1*Δ biological replicates using the Qiagen (Hilden, Germany) RNeasy isolation kit following mechanical disruption with 0.5 mm glass beads. Microarray analysis was performed in the Ramaciotti Centre for Genomics (University of New South Wales) using the Affymetrix GeneChip® Yeast Genome 2.0 Array. Microarray data were analyzed using R/Bioconductor (37), the '.CEL' data files imported using the affy package (1.52.0) (38). Scripts from Gillespie *et al.* (39) were used to mask the *S. pombe* probes, to extract the data for the *S. cerevisiae* probes. The intensity values from the *S. cerevisiae* probes were normalized using the Robust Multi-array Average (RMA) (40) function from the affy package. The quality of the normalized data were assessed using arrayQualityMetrics (v3.30.0) (39). Scripts from Gillespie *et al.* (39) were used to compute the average normalized values from multiple probes of the same gene. The differential expression of genes between the *hmt1*Δ and wild-type control yeasts was analyzed using limma (v3.30.4) (41). The Remove Unwanted Variation (RUV4) tool (v0.9.6) (42) was used to remove unwanted variation from the microarray data, with 500 of the least differentially expressed genes identified from an initial limma analysis used as empirical negative control genes. Two unwanted factors identified using RUV4 were removed using the linear model and a subsequent limma analysis was used to identify a final set of differentially expressed genes. The p values were adjusted using the Benjamini-Hochberg procedure.

Protein Extraction, 1-D Gel Electrophoresis, and Immunoblotting—Cells were harvested, lysed, and proteins electrophoresed according to previous methods (43). Immunoblotting was performed according to Low *et al.* (4). Primary and secondary antibodies used in this study, and their conditions of use, are detailed in supplemental Table S1.

SILAC Mass Spectrometry—For SILAC experiments, lysates were mixed prior to 1-D gel electrophoresis. Resulting gel lanes were excised into 13 slices according to protein mass; these were then reduced and alkylated prior to in-gel tryptic digestion according to established methods (44). The peptide digest pool was vacuum-dried (Savant SPD1010, Thermofisher Scientific, Waltham, MA) before resuspending in 20 μl of 0.1% (v/v) formic acid for mass spectrometric analysis. LC-MS/MS analysis of extracted peptides were performed twice on an LTQ Orbitrap Velos Pro (Thermo Fisher Scientific) using an UltiMate 3000 HPLC and autosampler system (Dionex, Sunnyvale, CA) according to previous methods (6).

Sequence Database Search and SILAC Data Analysis—For SILAC samples, raw files were processed using MaxQuant software (version 1.3.0.5) (45) using the Andromeda search engine, searching against the UniProtKB yeast database (July 2013, 6729 entries) (46). Search parameters were as follows: digestion with trypsin, variable modifications of methionine oxidation, serine-threonine-tyrosine phosphorylation and cysteine carbamidomethylation, peptides of minimum six or more amino acids, maximum of two missed cleavages, minimum two razor peptides for quantitation, and peptide and protein false discovery rate of 0.01. No fixed modifications were used. For search tolerances, MS1 was set to < 5 ppm and MS2 was set to 0.40 Da.

Functional Analysis of Differentially Expressed Genes and Proteins—Gene ontology (GO) terms for all differentially abundant proteins or differentially expressed genes, from proteomics and RNA-Seq experiments respectively, were extracted and overrepresented functional categories were determined by use of GOMiner (47). All unique identified proteins and genes served as the background list, and level 4 GO terms categories were examined, to find terms with a p value of < 0.05.

Experimental Design and Statistical Rationale—To determine the proteome-level consequences of the deletion of *HMT1*, four parallel cultures (two of each of the background strain and *hmt1*Δ in heavy and light media) were used in SILAC experiments, producing two biological replicates. After the normalization of protein ratios in MaxQuant (45), the resultant data set of ~1500 proteins with quantitative information was then subjected to filtering, prior to any statistical analysis. The following rules were applied:

a) If a protein was identified with three or more peptides, any peptides with ratios greater than two standard deviations away from the mean for that protein were considered outliers and excluded.

b) Proteins identified with less than two peptides were excluded.

c) Proteins identified in only one dataset (A or B) were excluded.

d) All contaminants (*e.g.* keratins, trypsin) were excluded.

Post-filtering, mean protein ratios were then recalculated for the remaining 1375 proteins, and re-normalized to 1.0 using the limma package in R/Bioconductor (37). Empirical Bayes-moderated p values for each protein were finally calculated in limma; this approach does not assume any fixed distribution of protein ratios.

For RNA-Seq, biological triplicates of wild-type and *hmt1*Δ yeast were grown, extracted and then analyzed by HiSeq 2000 next-generation sequencing. For microarray analysis, biological quadruplicates of wild-type and biological triplicates of *hmt1*Δ yeast were grown, RNA was extracted and then analyzed. Analysis of gene expression data was as detailed above.

Acid Phosphatase Assay—Extracellular acid phosphatase activity was quantified by the hydrolysis of p-nitrophenyl phosphate (pNPP) to p-nitrophenyl as per Lev *et al.* (48) or Orkwis *et al.* (49), with modifications. Cells from overnight cultures in YEPD were pelleted and washed twice in sterile water. To induce a response to high or low phosphate, cells were then resuspended in 4 ml MM-KH_2PO_4 or MM-KCl media at $OD_{600} = 1.0$ and incubated at 30 °C for 2 h. Next, cells were pelleted and resuspended in 3.2 ml of pNPP solution (2.5 mM pNPP (Sigma-Aldrich, St. Louis, MO) in 50 mM NaOAc, pH 5.2) and incubated at 37 °C. Every 30 min until 180 min, a 400 μl cell and pNPP aliquot was taken and mixed with 800 μl 1 M Na_2CO_3, cells were pelleted and p-nitrophenyl measured at OD_{420}. Two biological and two technical replicates were performed and data analyzed with Student's unpaired t test.

Polyphosphate Purification and Phosphate Quantification—The gene encoding the exopolyphosphatase of *S. cerevisiae* (ScPpx1p), with a 6× histidine tag at the C terminus, was overexpressed using the BG1805 overexpression plasmid in the yeast strain BY4741. Overexpression of proteins was induced overnight and 300 ml of culture was pelleted, resuspended in binding buffer (50 mM Tris-HCl buffer pH 8.0, 50 mM NaCl, 40 mM imidazole, 20% (v/v) glycerol, 0.25% (v/v) Triton X-100, supplemented with EDTA-free protease inhibitor (Roche, Basel, Switzerland)), lysed and clarified as described previously (43). Ppx1p was His-purified via 1 ml Ni NTA cartridges (Qiagen) precharged with Ni^{2+}-Sepharose for affinity purification ac-

cording to manufacturer's instructions. The final eluate was concentrated using the Amicon Ultra-4 10K centrifugal filter (Merck Millipore, Burlington, MA) at 25 °C and buffer exchanged with 50 mM Tris-HCl (pH 7.4), 200 mM NaCl to reduce NaCl to at least 200 mM and remove imidazole. Glycerol was added to a final concentration of 50% (v/v) before storage at −80 °C.

To monitor the cellular concentration of polyphosphates (polyP) in the wild-type and *hmt1*Δ mutant during growth, overnight cultures of cells were subcultured into fresh YEPD at $O.D._{600}$ = 0.2 and MM-KCl and MM-KH_2PO_4 at $O.D._{600}$ = 1.0. polyP was extracted at the lag (3 h from subculture), log (7 h) and stationary phases (10 h) of growth in YEPD as well as at 25 h after subculture. polyP in cells grown in MM-KCl and MM-KH_2PO_4 were extracted at the same harvesting times as for YEPD. Equal numbers of cells were adjusted by cell density for polyP extraction and purification and quantification were performed as described previously by Canadell *et al.* (50) with previously purified ScPpx1p.

To quantify total phosphate levels, cells were grown to $O.D._{600}$ = 1.0 in YEPD. Total phosphate levels were also quantified from MM-KCl and MM-KH_2PO_4 after 3 h of subculture from YEPD at a starting $O.D._{600}$ = 1.0. Equivalent numbers of cells were washed with sterile Milli Q water, boiled in 1 M H_2SO_4 for 20 min and assessed using P_i ColorLock™ Gold (Innova Biosciences, Cambridge, UK) according to manufacturer's instructions. Both polyphosphate and total phosphate quantification assays were performed with two technical replicates in at least three biological replicates.

Expression and His-purification of Pho2p and Pho4p—PHO2 and *PHO4* were cloned from BG1805 plasmids (Thermo Fisher Scientific) into pRsfT25MCS1 (51) (see supplemental Table S2 for plasmids) using PhoLinkF and PhoR primers specific for *PHO2* and *PHO4* respectively (see supplemental Table S3 for primers). The vector pRsfT25MCS1 was amplified using DuetPstF and DuetHisRLink primers. *PHO2* and *PHO4* were cloned separately into the vector using Gibson assembly cloning kit (New England Biolabs, Ipswich, MA), according to manufacturer's instruction. Assembled plasmids were transformed into Alpha-select Gold efficiency competent cells (Bioline, London, UK). Transformants were plated onto LB plates with 50 μg/ml kanamycin for selection. Successful assembly was screened with PCR using T7 promoter and DuetDOWN1 primers (supplemental Table S3) and confirmed with Sanger sequencing.

Plasmids were grown, extracted and then transformed into BL21 Rosetta (DE3) *E. coli* cells for protein expression. Plasmids carrying *HMT1* and *NPL3*, a known substrate of Hmt1p (52), were also transformed into the BL21 Rosetta (DE3) expression cells. All proteins were overexpressed by growing in LB at 37 °C with orbital shaking at 200 rpm and inducing expression of proteins by 1 mM IPTG. Protein induction was left for 6 h after which cells were pelleted and then lysed by cell sonication in binding buffer (50 mM Na-phosphate buffer pH 8.0, 0.5 M NaCl, 40 mM imidazole, 20% (v/v) glycerol, 0.25% (v/v) Triton X-100, 10 mM β-mercaptoethanol), supplemented with EDTA-free protease inhibitor (Roche). The lysates were clarified by centrifugation (16,000 × *g*, 20 min, 4 °C) and put onto HisTrap HP 1 ml columns (GE Healthcare, Chicago, IL). The final eluate was concentrated using centricon Plus-20 centrifugal column (Merck Millipore) at 4 °C, subjected to buffer exchange with 50 mM sodium-phosphate buffer pH 7.4, 0.2 M NaCl, 20% (v/v) glycerol and stored as detailed previously.

Immunoprecipitation of Chromosomally GFP Tagged Pho4p—The Pho4p-GFP strain was cultured in MM-KCl or MM-KH_2PO_4 to induce a high and low phosphate response, as above, before the Pho4p-GFP fusion protein was immunoprecipitated using GFP-Trap®_MA (ChromoTek, Munich, Germany). Cells were lysed in lysis buffer (10 mM Tris-Cl pH 7.5, 150 mM NaCl, 0.5 mM EDTAm 0.5% Triton X-100, 2.5 mM $MgCl_2$, 20 U/ml DNase (New England Biolabs), cOmplete™ mini EDTA-free protease inhibitor (Roche), and PhoSTOP™ phosphatase inhibitor (Roche)) by bead-beating 3 times for 30 s with 3 min incubations on ice between steps. Lysates were then clarified (21,000 × *g* for 40 min at 4 °C) and filtered through a 0.45 μm filter. 25 μl of GFP-Trap®_MA bead slurry was washed three times with 500 μl chilled wash buffer (10 mM Tris-Cl pH 7.5, 150 mM NaCl, 0.5 mM EDTA) before 2.5 mg of lysate was added to beads and incubated for 1 h at 4 °C with end-over-end mixing. Beads were washed three more times before boiling in 50 μl 2× SDS-PAGE sample buffer for 10 min. Eluates were separated by 1-D electrophoresis and the band corresponding to Pho4p-GFP was analyzed by mass spectrometry as described below.

In Vitro and In Vivo Methylation and ETD-MS/MS Analysis—All assays were performed essentially as described in (27), using recombinantly generated Hmt1p (53). Methylation reactions were incubated at 30 °C for 2 h. Negative controls for each reaction were performed with the omission of SAM (S-adenosyl methionine) in a replicate reaction, substituted with water. Electron transfer dissociation (ETD) analysis of *in vitro* protein methylation was conducted on an LTQ Orbitrap Velos Pro ETD (Thermo Fisher Scientific) as described previously (53). MS-Digest (version 5.19.1, University of California, San Francisco) outputs were used to calculate theoretical *m/z* values associated with doubly and triply charged arginine methylated peptides; these *m/z* values were incorporated into LC-MS/MS inclusion lists for use in mixed targeted and data dependent acquisition LC-MS/MS experiments. Theoretical Pho2p or Pho4p peptide masses were generated in MS-Digest using the following parameters: trypsin digest (up to two missed cleavages); variable modifications of carbamidomethyl (C), Methyl (R), Dimethyl (Uncleaved R), Oxidation (M), Phospho (STY); peptide masses 700 to 8000; and a minimum peptide length of 5. No fixed modifications were used.

For analysis of *in vitro* protein methylation data, files were submitted to the database search program Mascot (version 2.3, Matrix Science). Searches and verification of methylpeptides by manual examination for neutral losses were performed according to (5): instrument type was set as ETD-TRAP; precursor and MS/MS tolerances were ±4 ppm and ±0.4 Da, respectively; variable modifications of acrylamide (C), carbamidomethyl (C), oxidation (M), methylation (R) and demethylation (R) was used; digestion with trypsin was specified with two or four allowed missed cleavages; and the SwissProt database was searched. No fixed modifications were used. For the validation of *in vitro* methylated peptide of Pho4p, a peptide of sequence R_{met}SSGALVDDDKR was chemically synthesized (ChinaPeptides, Shanghai, China) and analyzed as above. Analysis of *in vivo* methylation of Pho4p involved the overexpressing the His-tagged protein on a BG1805 plasmid in wild-type BY4741 yeast. This and the affinity purification of Pho4p was done according to (54). The resulting protein, as well as Pho4p-GFP immunoprecipitated as described above, were prepared for mass spectrometric analysis as described previously (53). Peptide samples were analyzed using an UltiMate 3000 HPLC and autosampler system (Dionex) coupled to a Fusion Lumos Tribrid (Thermo Fisher Scientific). Nano-LC and nano-ESI were performed following experimental procedures described previously (53). Survey scans *m/z* 350–1750 were acquired in the Orbitrap (resolution = 120,000 FWHM) with an AGC target value of 4×10^5 charges (maximum ion injection time = 50 ms). Peptide ions (>5000 counts) with charge states of 2–8 were sequentially isolated and fragmented via ETD performed with a 100 ms reaction time, supplemental activation employed (ETciD at 10% collision energy) and a fluoranthene anion target of 6×10^5. Fragment ions were mass analyzed in the linear ion trap. Dynamic exclusion was applied to ions subjected to MS/MS using the following parameters: exclude after $n = 1$, exclusion duration = 25 s and mass tolerance = 10 ppm. A mixed targeted and

data dependent acquisition approach was employed using inclusion lists generated following the methods described above.

Site-directed Mutagenesis of PHO4 and HMT1—The Arg-241 (R241) of Pho4p was mutated to lysine in pRsfT25MCS1-Pho4 (supplemental Table S2). This was performed by use of Site-directed Ligase Independent Mutagenesis (SLIM) developed by Chiu *et al.* (55) with primers listed in supplemental Table S3. Plasmids were mixed and subjected to DpnI restriction enzyme digestion (New England Biolabs) to eliminate template DNA. Ten microliters from each PCR reaction were combined and hybridized. A hybridization program consisting of a denaturing step at 99 °C for 5 min, 3 cycles at 65 °C for 5 min and 30 °C for 45 min was used. The hybridization products were transformed into Alpha-select Gold efficiency competent cells (Bioline) at 5 μl of hybridization product per 50 μl of competent cells. Verification of the SLIM-modified plasmids was performed via colony PCR screening followed by Sanger sequencing. Next, mutated *PHO4* gene was amplified from pRsfT25MCS1 using Pho4_Fwd145 and Pho4_Rev173 primers, whereas G68R *HMT1* was amplified from DuetHmt1G68R-Npl3T18 (51) using Hmt1_Fwd145 and Hmt1_Rev173 primers (supplemental Table S3). Separately, the vector pRS426, containing *URA3* marker, was amplified using p426_Fwd173 and p426_Rev145 primers. The fragments were assembled using Gibson assembly cloning kit (New England Biolabs), subjected to DpnI digestion, plasmid hybridization as above, and then screened for successful incorporation of mutated *PHO4* or *HMT1* into pRS426 using p426Ura primers. Subsequently, mutated *PHO4* or *HMT1* was amplified alongside *URA3*, using Fwd_Pho4/Rev_Ura3 or Fwd_Hmt1/Rev_Ura3_Hmt1 primers, respectively, containing flanking regions upstream and downstream of transformation target site as described in (28). The PCR products were transformed into wild-type *S. cerevisiae* as described in (56) and plated onto SC-URA plates (0.192% (w/v) yeast synthetic drop-out without uracil (Sigma-Aldrich), 0.17% (w/v) yeast nitrogen base without amino acids and ammonium sulfate (BD Biosciences), 0.5% (w/v) ammonium sulfate, 2% (w/v) D-glucose, 2% (w/v) agar). DNA was extracted from successful transformants, screened with Pho4_A/Pho4_D or Hmt1_Check_A/Hmt1_Check_D primers, and finally confirmed with Sanger sequencing.

Fluorescence Microscopy—Low phosphate YEPD (1% (w/v) yeast extract, 2% (w/v) bacteriological peptone, 2% (w/v) D-glucose and 0.246% (w/v) $MgSO_4$ (pH 6.5)) was prepared by chelating phosphates with 8 ml of concentrated NH_4OH. After 30 min at room temperature, the solution was filtered twice through Whatmann paper before filter sterilization. Wild-type, Tef1p-GFP, Pho2p-GFP, Pho4p-GFP and *hmt1*Δ Pho2p-GFP and *hmt1*Δ Pho4p-GFP cells were grown overnight in YEPD, washed twice with water and resuspended in a 1:10 dilution of low phosphate YEPD with and without 10 mM KH_2PO_4. The cultures were incubated for 5–6 h at 30 °C with shaking. The localization of Pho4p was viewed in the specified growth media at room temperature under an inverted fluorescence microscope (Olympus IX71), fitted with a CoolSNAP HQ2/ICX285 camera (Photometrics, Tucson, AZ). For each strain, 20 images of representative cells were taken to quantify the nucleolar localization of Pho4p. Pho2p-GFP and Tef1p-GFP, which are proteins localized in the nucleus and cytoplasm, respectively, were included in fluorescence microscopy for comparison. Nuclei were stained by the addition of 1 μg/ml DAPI in the media for 20–30 min prior to viewing. Statistical analysis of Pho4p-GFP nuclear localization was performed using the student's unpaired *t* test, where $p < 0.05$ was considered significant.

Images were taken under an Olympus 100x OIL/1.40 objective. Image acquisition and deconvolution were performed with the Resolve3D softWoRx-Acquire (version 6.5.2) imaging software. Images were taken after 1 s of exposure, with a FITC filter for GFP fluorescence (475/28 nm excitation and 523/36 nm emission) and DAPI filter for nuclear fluorescence staining (390/18 nm excitation and 435/48 nm emission).

RESULTS

Transcriptome Analysis of hmt1Δ Yeast Reveals Downregulation of Genes Associated with Phosphate Homeostasis—To investigate the effects of Hmt1 gene deletion on the transcriptome, we first performed RNA-Seq analysis. Global gene expression in wild-type and *hmt1*Δ yeast at $O.D._{600} = 0.8–1.0$ was directly compared, with an average of 21.9 and 24.8 million reads generated for the biological triplicates of wild-type and *hmt1*Δ, respectively. Filtered RNA-Seq reads were aligned to the yeast genome and differential gene expression analysis performed using DESeq (36). A total of only 17 genes were found to be significantly differentially expressed between wild-type and *hmt1*Δ (Table I). Four genes showed up-regulation, whereas 13 genes including *HMT1* showed downregulation in *hmt1*Δ. *HMT1* showed more than a 1000-fold difference in read counts between wild-type and *hmt1*Δ yeast, confirming its knockout.

We investigated any functional relationships between differentially expressed genes using GOMiner (47). Six of the 17 genes were of unknown function. Analysis of the 11 remaining genes revealed that *acid phosphatase activity* and *phosphate metabolic process* were significantly downregulated (Fig. 1*A* and supplemental Table S4 for genes in each category). Genes involved were the acid phosphatases *PHO5*, *PHO11*, *PHO12*, the phosphate permease *PHO89* and cyclin-dependent kinase inhibitor *SPL2*. Interestingly, all are PHO (phosphate-responsive signaling) regulated and known to be controlled by transcription factor Pho4p (19). The *VTC3* member of the vacuolar transporter chaperone, involved in intracellular polyphosphate generation (19, 59, 60), was also significantly downregulated.

Validation of the *hmt1*Δ RNA-Seq data via microarray confirmed seven significantly downregulated genes that were also differentially expressed in RNA-Seq. These were *HMT1*, *FDC1*, *IMD2*, *SIZ1*, *SPL2*, *PHO11,* and *PHO5* (Table I). Additionally, other phosphate-associated genes were downregulated although their fold changes were not significant. These included *PHM6*, *PHM8*, *PHO3*, *PHO8*, *PHO84*, *PHO86*, *PHO89–91*, *VTC1–5,* and *IZH2* (61) (supplemental Fig. S1). Taken together, RNA-Seq and microarray analysis revealed a downregulation of the PHO pathway in *hmt1*Δ, raising the prospect that Hmt1p-mediated methylation affects phosphate homeostasis in the cell.

Deletion of HMT1 Leads to Downregulation of Proteins Associated with Phosphate Homeostasis—To determine if the gene expression changes in *hmt1*Δ affected the proteome, and in particular the PHO pathway, we used SILAC MS/MS. *S. cerevisiae* strain BY4741 *lys2*Δ/*arg4*Δ was used as background with critical steps in lysine and arginine biosynthesis knocked out to allow complete isotopic labeling. We then deleted the gene for methyltransferase Hmt1p in that back-

TABLE I

Differentially expressed genes in hmt1Δ compared to wild-type yeast during mid-log growth, analyzed by RNA-Seq and microarray

Genes are ranked by fold change, from greatest to smallest change.

Gene ID	Description	RNA-Seq analysis					Microarray analysis			
		Normalised count wild-type[a]	Normalised count *hmt1Δ*[a]	Fold Change (FC)	Log_2 (FC)	p_{adj}[b]	Normalised count wild-type[a]	Normalised count *hmt1Δ*[a]	Log_2 (FC)	p_{adj}[b]
Upregulated in *hmt1Δ*										
COS12	Uncharacterized protein	15.8	117.3	7.42	2.89	1.07E-16	7.7	8.3	0.53	5.15E-2
YFL067W	Uncharacterized protein	16.4	48.1	2.93	1.55	1.73E-02	7.3	7.5	0.20	8.55E-2
YHR214W-A	Putative uncharacterized protein	62.2	151.5	2.43	1.28	3.44E-04	–	–	–	–
SIZ1	E3 SUMO-protein ligase	221.2	532.8	2.41	1.27	5.84E-07	8.3	7.8	−0.52	3.86E-2
Downregulated in *hmt1Δ*										
HMT1	hnRNP arginine N-methyltransferase	2676.9	2.6	−1030	−10.02	5.38E-54	11.8	4.8	−7.06	1.12E-4
YGL118C	Putative uncharacterized protein	18.3	0.3	−61.0	−5.86	3.80E-06	–	–	–	–
PHO12	Repressible acid phosphatase	788.9	136.8	−5.78	−2.53	8.11E-23	–	–	–	–
SPL2	Putative CDK inhibitor	74.6	12.7	−5.87	−2.55	6.13E-10	11.8	11.5	−0.36	4.89E-2
PHO11	Repressible acid phosphatase	383.4	69.1	−5.55	−2.47	2.67E-19	13.3	12.2	−1.07	2.35E-2
IMD2	Inosine-5′-monophosphate dehydrogenase	1439.1	294.0	−4.89	−2.29	1.69E-26	9.3	7.9	−1.42	3.16E-2
YIR042C	Uncharacterized protein	177.6	47.8	−3.72	−1.89	2.61E-10	7.8	7.6	−0.28	1.04E-1
PHO89	Phosphate permease	68.5	25.1	−2.73	−1.45	5.12E-03	11.3	10.4	−0.95	6.25E-2
YER188W	Putative uncharacterized protein	99.5	39.2	−2.54	−1.34	1.75E-02	–	–	–	–
PHO5	Repressible acid phosphatase	423.2	209.8	−2.06	−1.01	1.24E-03	13.0	11.9	−1.05	6.49E-3
VTC3	Vacuolar transporter chaperone	1259.4	668.9	−1.88	−0.91	7.93E-02	13.1	12.9	−0.15	1.15E-1
FDC1	Ferulic acid decarboxylase	654.5	390.7	−1.68	−0.74	5.38E-02	9.9	9.5	−0.47	1.74E-2
YHR214C-B	Transposon Ty1-H Gag-Pol polyprotein	866.9	526.4	−1.65	−0.72	5.38E-02	–	–	–	–

[a]Mean normalized counts. [b]*p* values adjusted with the Benjamini–Hochberg procedure are as detailed in the DESeq package (36).

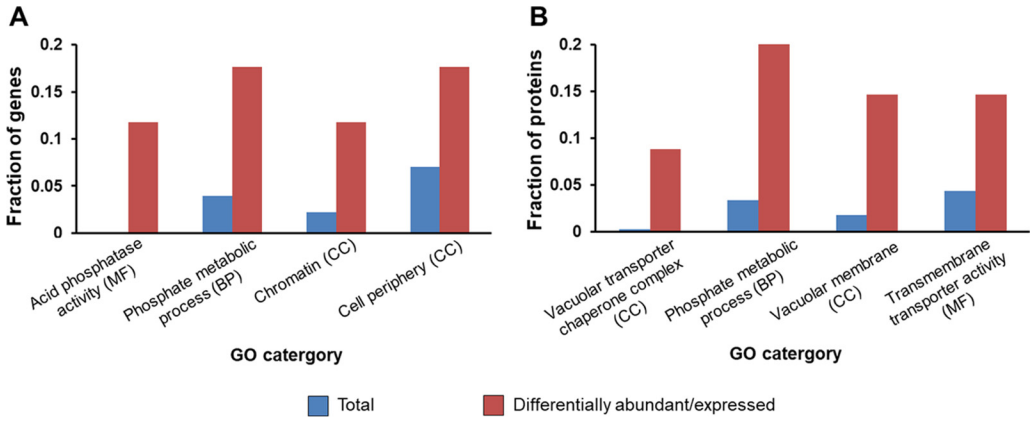

FIG. 1. **GOMiner functional enrichment analysis of differentially expressed genes and proteins in *hmt1*Δ, arising from RNA-Seq and proteomic analyses respectively.** *A*, The 17 genes identified as differentially expressed in RNA-Seq analysis were co-analyzed with all detected genes as background. *B*, The 32 differentially abundant proteins identified from SILAC MS/MS analysis were co-analyzed in a background of all 1375 proteins. Data information: Level 4 GO terms (cellular component, biological process, and molecular function) found to be most enriched ($p < 0.05$) are shown relative to total genes. GO = gene ontology; CC = cellular compartment; BP = biological process; MF = molecular function.

ground, to produce a *lys2*Δ/*arg4*Δ/*hmt1*Δ strain. A reciprocal SILAC design integrating an isotope label swap was used. Four parallel cultures (Fig. 2; each of the background and *hmt1*Δ strains in heavy and in light media) were grown to mid-log phase. We had previously determined that there was no discernible difference in growth rates between *hmt1*Δ and wild-type (supplemental Fig. S2). After harvest and lysis, protein extracts were combined and subjected to separation by SDS-PAGE. This produced two sets of biological replicates, A and B. We confirmed the completeness of metabolic labeling by analyzing single slices of light-labeled, heavy-labeled, and 1:1 mixed labeled lysates, using LC-MS/MS and MaxQuant. Heavy-labeled lysate showed isotope incorporation of ~97% (heavy peak intensity divided by light peak intensity, supplemental Fig. S3).

LC-MS/MS analysis was performed on an Orbitrap mass spectrometer with one iteration of exclusion list analysis. After MaxQuant (45) processing, there were ~1,900 proteins identified, and quantitative information attained for ~1,500 proteins. We subjected the quantitative data set to filtering prior to statistical analysis; the rules used for data filtering were as in the Experimental Design and Statistical Rationale. Postfiltering, mean protein ratios were recalculated for the remaining 1375 proteins, and B series ratios were inverted to match the A series ratios (*i.e.* a B ratio of 0.5 was converted to 2.0). Protein ratios for both series had distributions (supplemental Fig. S4) typical of SILAC analyses (62, 63). Statistically, we found 32 proteins to be of differential abundance between the background and *hmt1*Δ strains, where $p < 0.05$. Of the 32 proteins, 13 were of increased abundance in *hmt1*Δ whereas 19 showed decreased abundance (Table II). Interestingly, *VTC3*/Vtc3p were the only identical gene/protein pair that both showed significant downregulation. A lack of overlap in the genes/proteins of interest is not unexpected, given that the correlation between protein and mRNA levels can be

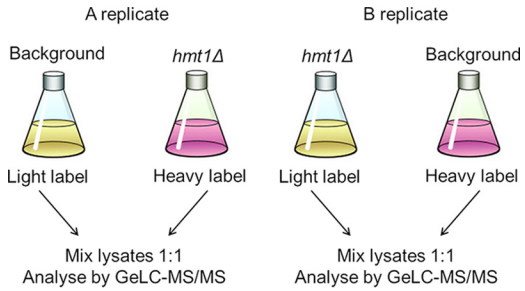

FIG. 2. **Schematic of reciprocal SILAC double-labeling experiment.** A replicate: Heavy/Light ratios > 1 indicates greater abundance in *hmt1*Δ. Heavy/Light ratios < 1 indicates greater abundance in background strain. B replicate: Heavy/Light ratios > 1 indicates greater abundance in background. Heavy/Light ratios < 1 indicates greater abundance in *hmt1*Δ.

poor (64). Several proteins of interest were unlikely to be detected by whole cell proteomics; for example, Pho5p, Pho11p and Pho12p are secreted extracellular acid phosphatases (65).

We investigated if there were functional relationships between the 32 differentially abundant proteins in *hmt1*Δ yeast (Table II). The GOMiner tool (47) was used to analyze these proteins, relative to a background of all identified proteins postfiltering. We found a significant enrichment of four functionally related categories. The category of *phosphate metabolic process* was enriched among the differentially abundant proteins in *hmt1*Δ (Fig. 1*B*), including the vacuolar transporter chaperone complex proteins (Vtc1p, Vtc3p, Vtc4p), the acid phosphatase Pho3p and the high-affinity phosphate transporter Pho84p (19, 59, 60). The category of *transmembrane transporter activity* also contained proteins associated with phosphate metabolism; Pho8p is a phosphatase (66) whereas Mir1p is a mitochondrial phosphate transporter (67). We noted that the vacuolar transporter chaperone complex proteins mapped to multiple categories, additionally being present in

TABLE II

Proteins exhibiting a significant change in abundance in hmt1Δ yeast, compared to background, as detected by SILAC MS/MS

Proteins are ranked by mean ratio, from greatest to smallest change.

Protein	Uniprot[a]	Description	Mean ratio[b]	Peptides (unique)[c]	*p* value[d]	Coverage[e]
Upregulated in *hmt1Δ*						
Psp2p	P50109	Uncharacterized protein	1.99	6 (6)	1.85E-02	15.3%
Scw4p	P53334	Probable family 17 glucosidase	1.78	2 (2)	1.42E-02	8.5%
Twf1p	P53250	Twinfilin-1	1.72	2 (2)	1.39E-02	9.0%
Arb1p	P40024	ABC transporter ATP-binding protein	1.58	20 (20)	3.40E-02	34.8%
Gar1p	P28007	H/ACA ribonucleoprotein complex subunit 1	1.48	2 (2)	1.29E-02	17.1%
Arg5,6p	Q01217	Protein ARG5,6, mitochondrial	1.41	22 (22)	2.14E-02	38.9%
Cmk1p	P27466	Calcium/calmodulin-dependent protein kinase I	1.39	4 (4)	2.12E-02	10.7%
Cue4p	Q04201	CUE domain-containing protein	1.38	3 (3)	2.57E-02	41.9%
Mir1p	P23641	Mitochondrial phosphate carrier protein	1.35	8 (8)	2.91E-02	43.7%
Atp17p	Q06405	ATP synthase subunit f, mitochondrial	1.34	5 (5)	4.76E-02	33.7%
Dbp2p	P24783	ATP-dependent RNA helicase	1.31	22 (22)	4.16E-02	43.6%
Bzz1p	P38822	Uncharacterized protein	1.3	3 (3)	4.86E-02	8.4%
YJL068C	P40363	S-formylglutathione hydrolase	1.3	4 (4)	4.57E-02	22.1%
Downregulated in *hmt1Δ*						
Vtc3p	Q02725	Vacuolar transporter chaperone	0.24	13 (13)	1.21E-03	18.1%
Pho84p	P25297	Inorganic phosphate transporter	0.3	3 (3)	2.27E-02	7.3%
Vtc1p	P40046	Vacuolar transporter chaperone	0.52	3 (3)	9.63E-03	14.7%
Vtc4p	P47075	Vacuolar transporter chaperone	0.57	17 (17)	1.38E-02	23.2%
Emp70p	P32802	Transmembrane 9 superfamily member 1	0.61	2 (2)	2.71E-02	6.3%
Pho8p	P11491	Repressible alkaline phosphatase	0.63	7 (7)	1.56E-02	19.3%
YLR413W	Q06689	Cell membrane protein	0.66	4 (4)	1.06E-02	5.6%
Pho3p	P24031	Constitutive acid phosphatase	0.69	5 (3)	3.93E-02	14.6%
Fpr4p	Q06205	FK506-binding protein 4	0.7	9 (8)	3.89E-02	30.2%
Pdr5p	P33302	Pleiotropic ABC efflux transporter of multiple drugs	0.72	14 (11)	3.23E-02	10.1%
Hem13p	P11353	Oxygen-dependent coproporphyrinogen-III oxidase	0.73	4 (4)	4.97E-02	15.2%
Fsh1p	P38777	Family of serine hydrolases 1	0.73	6 (6)	2.35E-02	34.0%
Bat2p	P47176	Branched-chain-amino-acid aminotransferase, cytosolic	0.73	11 (8)	3.40E-02	27.4%
Lsb5p	P25369	LAS seventeen-binding protein 5	0.74	2 (2)	3.41E-02	8.5%
Lrg1p	P35688	Rho-GTPase-activating protein	0.75	3 (3)	3.62E-02	3.6%
YJR029W*	P47100	Transposon Ty1-JR2 Gag-Pol polyprotein	0.75	45 (0)	3.17E-02	33.4%
Lac1p	P28496	Sphingosine N-acyltransferase	0.75	3 (3)	4.44E-02	12.0%
Dbp10p	Q12389	ATP-dependant RNA helicase	0.76	3 (3)	3.72E-02	4.8%
Hxt3p	P32466	Low-affinity glucose transporter	0.77	6 (5)	4.31E-02	12.6%

[a]Uniprot accession number of protein. [b]Average (mean) ratio of both A and B replicates. [c]Peptides identified from protein, unique peptides in brackets. [d]Proteins with abundance differences of $p < 0.05$, Bayes-moderated. [e]Peptide sequence coverage of identified protein.

*Peptides common to Q12414; Q03612; P0C2I3; P0C2I5; P0C2I7; Q04214; Q12490; P0C2I9; P47100; P0C2J0; Q04670; P0C2I2; Q04711; Q92393; O13535; Q03619; Q12088; Q12316; Q12193.

the enriched cellular compartments of *vacuolar membrane* and *vacuolar transporter chaperone complex*. A list of the differentially abundant proteins found in each enriched functional category is presented in supplemental Table S5.

Phosphate regulation and metabolism is controlled by the PHO (phosphate-responsive signaling) pathway in yeast (68). The vacuolar transporter chaperone (VTC) proteins are known to be induced under low-phosphate conditions, as are the Pho84p phosphate transporter and the Pho8p vacuolar phosphatase (19). All are under the control of the Pho4p transcriptional activator. The fact that these PHO-regulated proteins uniformly displayed a decreased abundance in *hmt1Δ* suggests PHO pathway repression, as was also seen in the gene expression analysis. It is notable that three of the four proteins of the VTC complex (Vtc1p, Vtc3p, Vtc4p) demonstrated decreased abundance in *hmt1Δ*. The VTC complex plays a crucial role in phosphate homeostasis as part of the PHO pathway (19, 69, 70). The VTC complex is present on the endoplasmic reticulum, at vacuoles, and the cell periphery, but is enriched at the vacuolar membrane (71). The Emp70p and Pho8p proteins, significantly downregulated as per Vtc1p, Vtc3p, Vtc4p, also localize to this cellular component (72, 73).

Some Hmt1p Substrates Display Changed Protein Abundance but Are Unchanged at Transcript Level—Comparatively few proteins (13 out of 32) displayed an increase in abun-

dance in *hmt1*Δ yeast (Table II). Three of these 13 proteins were of interest as they are either known or putative substrates of the methyltransferase Hmt1p (4), however it is notable that there was no significant increase or decrease in transcript levels of these or any other known or putative Hmt1 substrate. Gar1p has been shown to be methylated by Hmt1p (5, 74), whereas Psp2p and Dbp2p have been proposed as substrates of Hmt1p because of the presence of RGG-rich regions (75). To further investigate the increase in abundance of Hmt1p substrates, we subjected yeast strains carrying TAP-tagged Gar1p and Dbp2p to *HMT1* knockout. One-dimensional SDS-PAGE and immunoblotting validated an increased abundance of Dbp2p in *hmt1*Δ (supplemental Fig. S5). This suggests the regulation of Dbp2p abundance at the protein level. However, Gar1p in *hmt1*Δ yeast was found to migrate anomalously because of the absence of arginine methylation, appearing as a band of lower mass (supplemental Fig. S5).

Network Analysis Reveals No Associations Between Known Hmt1p Substrates and Phosphate Regulation—It was not immediately apparent how deletion of *HMT1* could affect the regulation of phosphate in the yeast cell. No known Hmt1p substrates showed any differences in gene expression, whereas the above-mentioned Dbp2p, Gar1p and Psp2p proteins have no known association with the regulation of phosphate. Given that arginine methylation can modulate protein-protein or protein-RNA interactions (52, 76) we first examined networks of physical and functional interactions in the STRING database (77) for evidence of interactions between known substrates of Hmt1p and the differentially expressed genes/differentially abundant proteins. As Hmt1p is known to methylate many RNA-binding heterogeneous nuclear ribonucleoproteins (hnRNPs), it was not surprising that several of our differentially expressed transcripts have been reported to interact with known Hmt1p substrates Nab2p and Sbp1p (supplemental Fig. S6). However, Nab2p is a general RNA-binding protein, involved in nuclear export of over 2500 mRNAs (78). Similarly, Sbp1p has been reported to interact with $>$ 1000 different RNAs (79). These interactions are therefore not specifically associated with phosphate regulation. Though not revealed in the STRING analysis, several our differentially expressed genes/differentially abundant proteins have been reported to interact with Hmt1p substrates. Siz1p has been reported to interact physically with Nab2p and Tif4632p, another putative substrate of Hmt1p (81). However, there is no evidence of those interactions being methylation-dependent. Interestingly, transcripts *YFL067W* and *YHR214W-A* have been reported to bind Hek2p (82). Although Hek2p is not known to be a substrate of Hmt1p, or reported to carry arginine methylation in yeast, its human homolog hnRNP K has been reported to be methylated at five sites by PRMT1, the human equivalent of Hmt1p (83). Notwithstanding these observations, there was no apparent functional association between phosphate regulation and known substrates of Hmt1p that had differentially expressed genes or differentially abundant proteins.

HMT1 Knockout Yeast Shows Decreased Acid Phosphatase Activity and Lower Total P_i Levels—During mid-log growth, *hmt1*Δ showed a decrease in expression or abundance of genes and proteins associated with phosphate regulation and metabolism (Tables I and II, Fig. 1). These included repressible acid phosphatase family proteins (*PHO5, PHO11,* and *PHO12*), high-affinity phosphate transporters (Pho84p and *PHO89*), subunits of the VTC complex associated with polyP accumulation (Vtc1p, Vtc3p, and Vtc4p), and *SPL2* - a gene whose product affects the localization of the Pho87p low affinity phosphate transporter (84). Accordingly, we investigated whether there was any change in extracellular acid phosphatase activity, along with total P_i and inorganic polyphosphate (polyP) stores between *hmt1*Δ and wild-type yeast.

To assay extracellular acid phosphatases, wild-type and *hmt1*Δ cells were first grown in YEPD and then conditioned in phosphate depleted (MM-KCl) or phosphate replete (MM-KH_2PO_4) media. Cells were then washed prior to the pNPP hydrolysis assay. Compared with the wild type, *hmt1*Δ showed a ~33% reduction ($p < 0.05$) in pNPP hydrolysis when cells were first conditioned in either phosphate depleted or phosphate replete media (Fig. 3*A*). This indicates a significant decrease in extracellular acid phosphatase activity. A longer conditioning also showed a similar trend (supplemental Fig. S7). These observations validated the gene expression results (Table I), in which *hmt1*Δ showed a significant down-regulation in the genes of secreted acid phosphatases *PHO5, PHO11,* and *PHO12*. To determine that the loss of enzymatic activity of Hmt1p was the cause of the decreased acid phosphatase activity, we also assayed a strain where we had engineered the G68R mutation into the chromosomal gene for Hmt1p. This mutation generates an inactive version of the enzyme (52, 85). The inactive G68R Hmt1p showed similar decreases in extracellular acid phosphatase activity as the *hmt1*Δ strain (Fig. 3*A*), indicating that loss of Hmt1p activity and not just the loss of the Hmt1p protein itself causes a decreased level of extracellular acid phosphatases.

Total P_i was extracted and quantified from wild-type and *hmt1*Δ cells grown in phosphate depleted, phosphate replete or YEPD media (Fig. 3*B*). The *hmt1*Δ cells showed a significant 30% reduction ($p < 0.0001$) of total P_i levels, as compared with wild-type, when both were grown in phosphate depleted media. This likely reflects the lower abundance of the high affinity phosphate transporter Pho84p in *hmt1*Δ, as seen in the proteomic analysis (Table II). Differences in response to different media were also seen, in that wild-type cells showed a significant 30% decrease ($p < 0.0001$) in total P_i when grown in phosphate replete MM-KH_2PO_4 medium compared with phosphate depleted MM-KCl. In contrast, *hmt1*Δ cells exhibited no significant changes in P_i levels between phosphate replete and depleted media. No differences

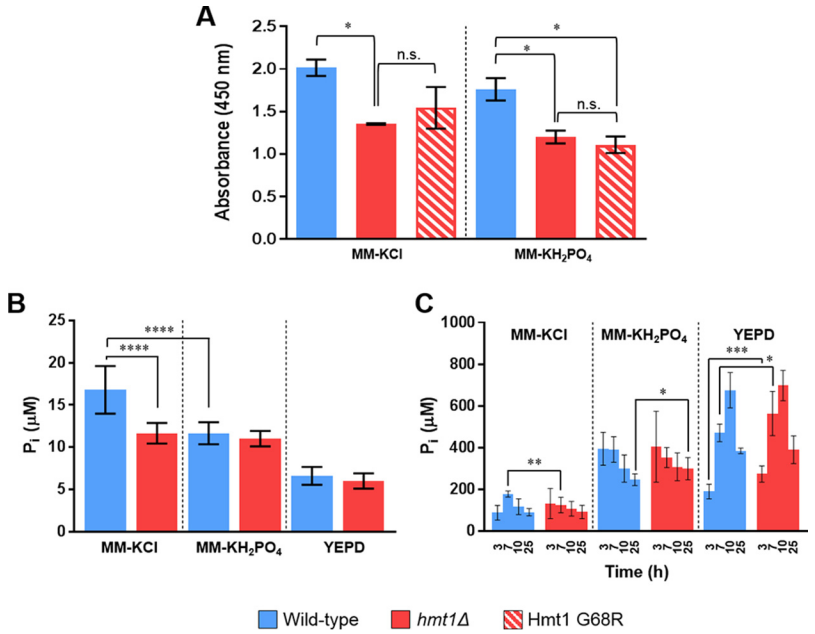

FIG. 3. **The *hmt1*Δ mutant shows dysregulation of phosphate metabolism.** *A*, The *hmt1*Δ mutant has significantly lower extracellular acid phosphatase activity compared with wild-type, after 2 h's conditioning in phosphate depleted (MM-KCl) or phosphate replete (MM-KH_2PO_4) media. Assay results are at time 180 min, after adding cells to the pNPP reaction mix. *B*, The *hmt1*Δ mutant shows lower total P_i compared with the wild-type in phosphate depleted medium (MM-KCl). No differences in total P_i were observed for *hmt1*Δ between low (MM-KCl) and high phosphate (MM-KH_2PO_4) media, however the wild-type did show a significant decrease between these two conditions. *C*, The *hmt1*Δ mutant, compared with wild-type, shows significant changes in polyP levels at some phases of growth in MM-KCl, MM-KH_2PO_4 and YEPD. Time 3 h is lag, 7 is log, 10 is stationary and 25 h is overnight. Data information: Data are presented as mean and error bars indicate standard deviation. Mean was obtained from at least two biological replicates. In A, B and C, * indicates $p < 0.05$, ** indicates $p < 0.002$, *** indicates $p < 0.0005$ and **** indicates $p < 0.0001$ (Student's unpaired *t* test).

in P_i levels were found between wild-type and *hmt1*Δ grown in YEPD (which has a higher concentration of phosphate than MM-KCl and has higher nutrients).

Finally, polyP abundance between wild-type and *hmt1*Δ cells was examined when cells were subcultured from YEPD to different media; this is known to affect polyP synthesis and accumulation (86). Accordingly, we compared the polyP accumulation between wild-type and *hmt1*Δ that were first grown in YEPD and then subcultured to either phosphate depleted, phosphate replete or YEPD media. polyP accumulation was examined at the lag, log, stationary and overnight stages of growth (Fig. 3*C* and supplemental Fig. S8), by enzymatic hydrolysis of polyP to P_i with purified exopolyphosphatase Ppx1p. Upon transfer of cells to phosphate depleted medium (MM-KCl), we observed low overall polyP levels and little accumulation of polyP from lag through to stationary phase in wild-type or *hmt1*Δ (86). However, compared with the wild-type, *hmt1*Δ showed a significant decrease in polyP levels at the log phase ($p = 0.0023$). Upon transfer of cells from YEPD to phosphate replete medium (MM-KH_2PO_4), successful accumulation of polyP was evident in wild-type and *hmt1*Δ cells (as seen by overall higher P_i as compared with MM-KCl). This is consistent with previous reports (87). Despite the downregulation of VTC genes and proteins in *hmt1*Δ cells (Tables I and II), which are involved in polyP synthesis (19), a significant increase in polyP concentration in *hmt1*Δ was observed compared with the wild-type after growth overnight ($p = 0.0464$). Upon transfer of cells from YEPD to fresh YEPD, wild-type and *hmt1*Δ cells from lag to stationary phase showed an expected increase in polyP levels (86). Contrary to VTC regulation (Tables I and II), however, a significant increase in polyP concentration was observed in *hmt1*Δ compared with the wild-type in the lag ($p < 0.0005$) and log ($p = 0.0361$) phases.

Pho4p Is An In Vitro Substrate of Hmt1p with A Single Arginine Methylation Site at Arg-241—Our studies of gene and protein expression in *hmt1*Δ, and the analysis of extracellular phosphatases and intracellular P_i, highlighted a dysregulation in phosphate homeostasis. Given that many of the genes are regulated by transcription factor Pho4p, which undergoes nucleocytoplasmic shuttling, and given that Hmt1p methylation can mediate nuclear exit of proteins (88, 89), we investigated whether Pho4p is a substrate of Hmt1p. We also examined whether Pho2p, which complexes with Pho4p for activation of gene expression, is a substrate of Hmt1p.

Recombinant Hmt1p, Pho2p and Pho4p were purified from *E. coli* and used in *in vitro* methylation assays. Purified Npl3p, a known substrate of Hmt1p (90), was used as a positive

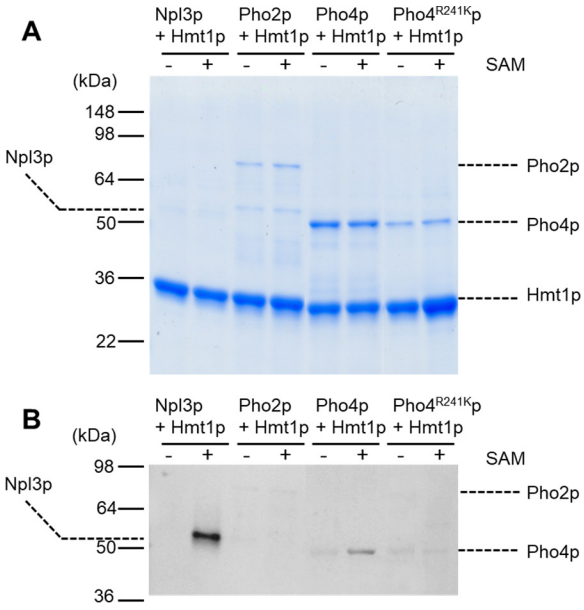

FIG. 4. **Pho4p, but not Pho2p, is an *in vitro* substrate of Hmt1p.** *A*, Coomassie-stained gel of *in vitro* methylation assay samples. Methylation of Pho4p was seen on the addition of Hmt1p and the methyl donor SAM, but lost when the monomethylarginine site, Arg-241, was mutated to lysine. Npl3p, a known substrate of Hmt1p, was used as a positive control. Reactions omitting SAM were negative controls. *B*, The corresponding immunoblot of *in vitro* methylation assay samples, probed with anti-monomethylarginine antibody. Methylation is present on Npl3p and Pho4p with the presence of Hmt1p and addition of SAM, but not on Pho2p and mutated Pho4p.

control, whereas reactions omitting the methyl group donor SAM were negative controls. The samples were then subjected to gel electrophoresis and immunoblotting with an anti-mono-methylarginine primary antibody. Interestingly, this indicated that Hmt1p could catalyze the methylation of Pho4p *in vitro* (Fig. 4). By contrast, Pho2p showed no methylation with or without the presence of SAM, indicating that it was not methylated by Hmt1p. As expected, the positive control Npl3p was successfully methylated by Hmt1p and Pho4p was not methylated in the negative control.

To characterize the type and site(s) of methylation, we analyzed *in vitro* methylated Pho4p by ETD-MS/MS. This revealed mono-methylation on Arg-241, on a peptide of sequence R_{met}SSGALVDDDKR (Fig. 5). This peptide, and its modification, was validated by chemically synthesizing the same peptide and comparing its fragmentation spectra with the native counterpart. Both peptides showed near-identical fragmentation and neutral losses characteristic of arginine monomethylation (Fig. 5*B*). To investigate whether only one amino acid of Pho4p is subject to methylation, site-directed mutagenesis was performed, whereby Arg-241 in recombinant Pho4p was substituted to lysine to generate Pho4p R241K. An *in vitro* methylation assay showed that this mutant protein could not be methylated by Hmt1p, as detected by immunoblotting (Fig. 4*B*).

We investigated the Arg-241 monomethylation site *in vivo*, for its presence and possible function when mutated to lysine. Overexpressed, His-tagged Pho4p from wild-type yeast was purified and analyzed by ETD-MS/MS. Unexpectedly, this did not reveal the presence of arginine methylation at Arg-241 (supplemental Fig. S9). A chromosomal GFP fusion of Pho4p (29) was also immunoprecipitated and analyzed by MS/MS. Although expressed at native abundance, this also did not reveal the presence of methylation at Arg-241, although it should be noted that the peptides covering this region of Pho4p were detected at low levels (supplemental Fig. S10). Phosphosites at Ser-242 and Set-243 were, however, confirmed (supplemental Figs. S9 and S10). Finally, we mutated Arg-241 to lysine in the chromosomal *pho4* gene and assayed extracellular acid phosphatase levels compared with wild type. This was done in MM-KCl and in MM-KH_2PO_4. This revealed a dysregulation of extracellular phosphatase activity (supplemental Fig. S11) although as a significant increase compared with wild type ($p < 0.05$) in MM-KCl. This was unexpected as a significant decrease in activity was seen in *hmt1*Δ cells under the same conditions (Fig. 3*A*).

HMT1 Knockout Does Not Affect Nuclear Localization of Pho4p Under Phosphate Limitation—It is known that Pho4p multimerizes with Pho2p to activate the transcription of genes involved in the PHO regulatory pathway (91). Pho4p is localized to the nucleus and the cytoplasm in phosphate depleted and phosphate rich media, respectively (92). The shuttling of this transcription factor is dependent on its phosphorylation state, where the hypophosphorylation of Pho4p is critical to its nuclear localization (93). By contrast, Pho2p is localized in the nucleus and does not shuttle (94). As noted above, arginine methylation is known to be involved in the nucleocytoplasmic transport of Hmt1p substrates. The shuttling of Npl3p and Nab2p between the nucleus and the cytoplasm is methylation dependent (85, 88, 89, 95). Hence, we investigated whether the localization of Pho4p, being an *in vitro* substrate of Hmt1p, is affected by the loss of arginine methylation.

A strain containing chromosomally GFP-tagged Pho4p, previously used for the study of Pho4p localization (29), and one containing GFP-tagged Pho2p (96) were subjected to deletion of *HMT1*. GFP-tagged Tef1p (96) was used as a cytoplasmic localization control. We studied the localization of Pho2p and Pho4p fusion proteins in phosphate replete and depleted media. In both the wild-type and *hmt1*Δ mutant, there was no difference in Pho4p localization in either condition. Pho4p-GFP localized in the cytoplasm under replete phosphate and localized to the nucleus upon phosphate depletion (Fig. 6). Statistically, there was no significant difference in the level of Pho4p-GFP nuclear localization between the wild-type and knockout mutant (supplemental Fig. S12). As expected, the localization of Pho2p-GFP was nuclear in the wild-type and *hmt1*Δ mutant, whereas the localization of the control protein translational elongation factor Tef1p-GFP was cytosolic.

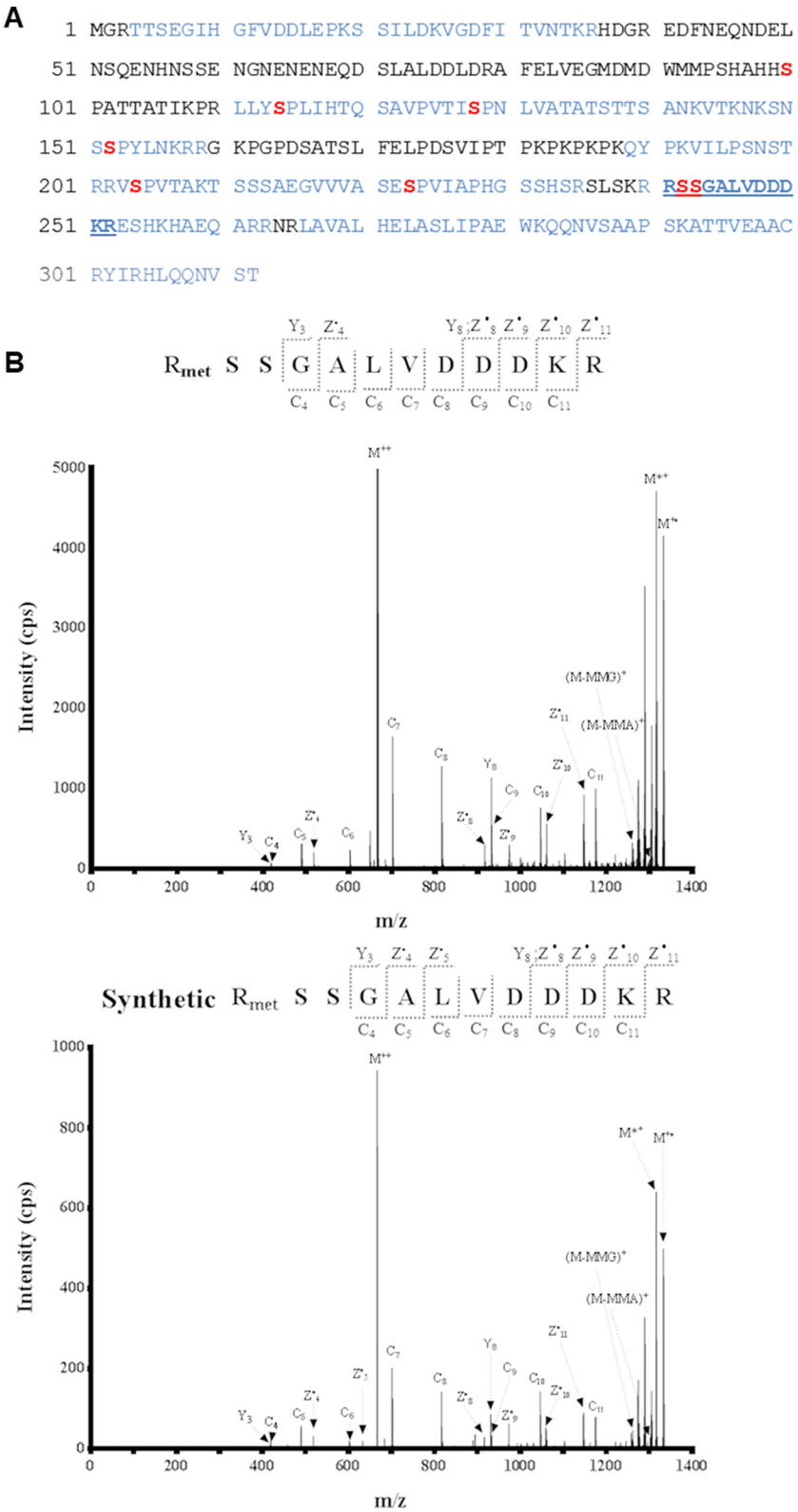

FIG. 5. **Hmt1p methylates Pho4p *in vitro* at Arg-241.** *A*, Protein sequence of Pho4p. The peptide carrying the mono-methylarginine site at position 241, discovered by ETD-MS/MS, is underlined and in bold blue. All other Pho4p peptides detected by ETD-MS/MS are blue. Regions shown in black were not detected in ETD-MS/MS; these included very large tryptic peptides at positions 41 to 79 (mass of 4520.8 Da), position 80 to 110 (mass of 3494.6 Da) and position 160 to 188 (mass of 3028.7 Da). Phosphorylation sites reported in the literature are shown in red.

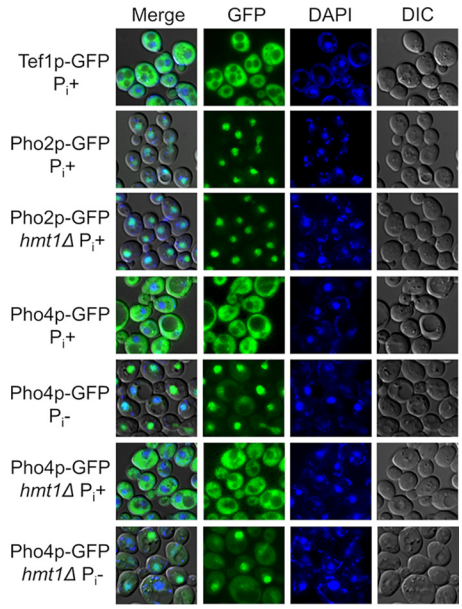

FIG. 6. **Deletion of *HMT1* has no effect on the nuclear localization of Pho4p-GFP under phosphate limited conditions compared with the wild-type.** Pho2p-GFP was localized to the nucleus, even with the deletion of *HMT1*, whereas Tef1p-GFP was localized in the cytoplasm. Images were taken at 100x objective (oil immersion).

DISCUSSION

Here we report that phosphate homeostasis in *S. cerevisiae* is disrupted through the deletion of *HMT1*. This was seen at both a transcriptomic and proteomic level; on deletion of *HMT1*, we observed a significant decrease in expression and abundance of many Pho4p target genes and their protein products. These included the genes *PHO5*, *PHO11*, *PHO12*, *SPL2*, *PHO89*, and *VTC3* (Table I) and proteins Pho3p, Pho8p, Pho84p, Vtc1p, Vtc3p, and Vtc4p (Table II) (19). Functionally, we found that these changes were associated with a reduction in the activity of component(s) of PHO regulation, especially but not only the decrease in extracellular acid phosphatase activity (Fig. 3*A*). We showed that this phenotype was also seen in a G68R mutant of Hmt1p, showing that the loss of Hmt1p activity, and not just a loss of the entire protein, leads to dysregulation of phosphate homeostasis. A decrease in total P_i levels was seen in *hmt1*Δ in low phosphate conditions (Fig. 3*B*). By contrast, the concentration of total P_i was similar between *hmt1*Δ and wild type in high phosphate media MM-KH_2PO_4 or in YEPD, which could reflect the accumulation of phosphate in cells through passive diffusion (97). Interestingly, although significant changes in polyP levels were observed in *hmt1*Δ compared with wild type (Fig. 3*C*), these were contrary to those expected, being a decrease in polyP concentrations in phosphate replete media YEPD and MM-KH_2PO_4 and increase in the phosphate depleted medium MM-KCl (86). This may be because of the VTC complex having functions separate to polyphosphate metabolism, such as vacuolar membrane fusion, V-ATPase activity and microautophagy (70, 71, 98).

In vitro investigation into Pho4p revealed that it could be monomethylated at arginine 241 by Hmt1p, in an RSS motif (Fig. 4 and 5). The motif is different to the canonical RGG motif for Hmt1p; noncanonical sites of Hmt1p methylation have been reported elsewhere (10, 11) although these too have arisen from *in vitro* experiments. Our analysis of Pho4p methylation *in vivo* was inconclusive as we did not detect methylation at Arg-241 or any other site, whether on a natively expressed GFP Pho4p fusion or on overexpressed Pho4p. However, it is possible that Arg-241 methylation only occurs under specific conditions, or is of low stoichiometry, and thus was undetected here. It is also possible that other regulatory relationships exist between arginine methylation and phosphorylation homeostasis in *S. cerevisiae* cell; a recent study reported the presence of polyphosphate on protein Nsr1p (99) which is a known *in vivo* substrate of Hmt1p (5).

The localization of some Hmt1p substrate proteins is known to be affected by methylation, including Npl3p, Hrb1p, Nab2p and Gbp2p (16, 74, 85, 89, 100). Knowing this, we investigated whether the loss of *HMT1* could affect the localization of Pho4p, interfering with the Pho4p nucleocytoplasmic shuttling that is dependent on its degree of phosphorylation (101). Using chromosomal GFP-fusions, we detected no change in the subcellular localization of Pho4p in the absence of *HMT1* (Fig. 6). This suggests that methylation of Pho4p, if confirmed *in vivo*, must affect phosphate regulation through mechanism(s) that affect the transcriptional activity but not localization of Pho4p.

The location of the putative arginine methylation site in Pho4p may provide clues to its function. There are two possible models for this. The first is that arginine methylation acts to increase the homodimerization of Pho4p or its binding affinity to DNA. To activate transcription of its target genes, Pho4p binds DNA as a homodimer with its basic helix-loop-helix (bHLH) motif, located at the C terminus (102). The methylation site at Arg-241 is located between the oligomerization and bHLH DNA-binding domains of Pho4p (Fig. 7). Based on the C-terminal crystal structure of Pho4p (103), the methylarginine is unlikely to be within the DNA-binding region. However, the proximity of Arg-241 to the oligomerization

B, The annotated ETD-MS/MS spectra for the methylated Pho4p peptide R_{met}SSGALVDDDKR from the *in vitro* methylation assay (top) and the synthetic methylated peptide (bottom) show near-identical fragmentation patterns, validating the identification of this methylarginine site on Pho4p. Summarized ion fragment coverages, where c- and z-ions and their derivatives are shown in each spectra. Precursor and charge-reduced precursor ions - c- and z-ions, which are prominent ions resulting from -NH_3 and methylarginine-associated losses - and their measured masses are labeled in the spectra. Methylarginine-associated neutral losses are abbreviated as follows: monomethylamine (MMA), monomethylguanidine (MMG). Losses from NH_3 are shown as '*'.

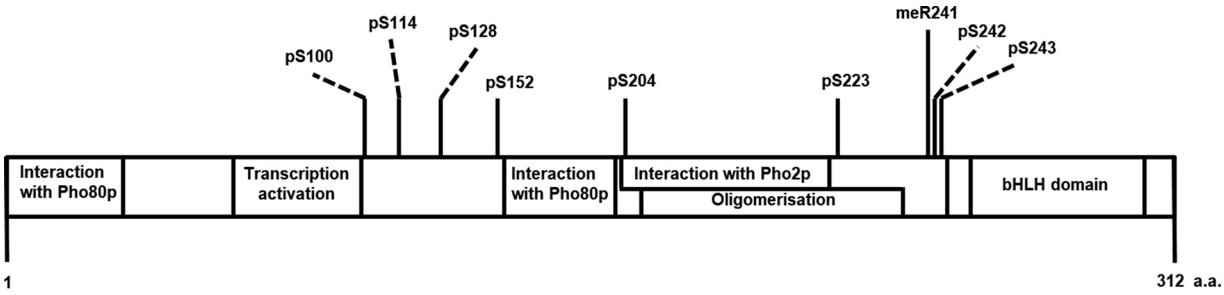

FIG. 7. ***In vitro* Pho4p methylation on Arg-241 is located between the oligomerisation and bHLH domains and is adjacent to two phosphorylation sites.** Schematic of Pho4p domains, mapped onto its total length of 312 amino acids. Domains are approximately to scale. Phosphosites and the *in vitro* Hmt1p-mediated methylation site are shown above the domain map.

and bHLH domains means its methylation could be involved in mediating the protein-protein interactions necessary for the activation of the target genes of Pho4p. There is a dimerization precedent in hnRNP protein Npl3p, where nuclear Hmt1p-mediated arginine methylation increases self-dimerization by ~2-fold (52, 104). The dimerization domain of Npl3p is in the C-terminal SR-domain, from positions 276–364, and loss of Npl3p dimerization results in defects in translation (105). We hypothesize that the function of the putative arginine methylation site on Pho4p could be like Npl3p, potentially increasing its homodimerization. If this is the case Pho4p could still dimerize in the absence of arginine methylation, albeit with lower affinity. This model could explain the significant reduction, but not complete loss of expression, of Pho4p target genes and proteins in *hmt1*Δ.

A second model for the putative Arg-241 methylation in Pho4p involves the interplay between phosphorylation and methylation. Interplay between modifications is emerging as a widespread means for the regulation of protein function, including in protein interaction codes (106). Pho4p is phosphorylated at eight different serine residues, five of which are phosphorylated by the Pho80p-Pho85p cyclin-CDK complex under high-phosphate conditions (92, 93). Four of these five phosphosites are well characterized in their respective roles: phosphorylation of Ser-114 and -128 signals nuclear export; phosphorylation of Ser-152 decreases nuclear import; and phosphorylation of Ser-223 decreases the binding affinity for Pho2p. The remaining three phosphoserines at positions 204, 242, and 243 are not phosphorylated by Pho85p, and their kinase(s) and molecular functions are unknown (107–109). It is noteworthy that the methylarginine site on Pho4p, reported in this study, is directly adjacent to the phosphoserines at positions 242 and 243 (Fig. 7) (109). Given its proximity to the DNA-binding domain, arginine methylation of Pho4p could potentially serve as a recruitment signal for transcriptional machinery, or to recruit kinases for the phosphorylation of Ser-242 and -243. A similar example involves the methylation of transcription factor STAT6 at Arg-27 (110), where the loss of arginine methylation leads to a decrease in IL4-dependent phosphorylation. Alternatively, given that all of the characterized phosphoserines in Pho4p inhibit its transcriptional activity (93), Pho4p methylation could serve to block this inhibition. In human cells, the methylation of Arg-296 and -299 by PRMT1 inhibited the phosphorylation of Ser-302 on hnRNP K, involved in chromatin remodelling, transcription, RNA splicing, mRNA stability and translation (111). Loss of methylation on these arginine residues led to an increase of p53-independent apoptosis upon DNA damage.

Post-translational modification of proteins, or combinations thereof, are important ways by which nutrient sensing can be controlled. Examples include the PHO pathway itself and, in mammalian cells, the interplay between O-linked β-N-acetyl glucosamine (O-GlcNAc) and phosphorylation (112). Our research has highlighted a possible new link between phosphate regulation and SAM levels, where SAM is the major methyl donor inside the cell. SAM is synthesized alongside phosphate and diphosphate from methionine and ATP by the S-adenosylmethionine synthetases Sam1p and Sam2p. Interestingly, the intracellular concentrations of SAM and phosphate are known to be correlated. The accumulation of SAM in the adenosine kinase mutant *ado1*Δ was accompanied by an upregulation in phosphate related transcripts and increased cellular concentrations of phosphate and polyP (113). Furthermore, polyP contributes to stability of SAM (113). The downregulation of the PHO regulon upon deletion of *HMT1*, revealed in our study, suggests an interdependency between the regulation of SAM and phosphate levels. Simplistically, this may be a means by which the cell does not expend resources on phosphate sequestration if there is not sufficient SAM to undertake a large range of other metabolic activities. This donor sensing and regulation of protein activity is like the dependence of acetyl-CoA donor levels on the activity of lysine acetyltransferases (KATs), which acetylate enzymes that regulate various metabolic processes in the cell (114). In conclusion, this study has shown that loss of Hmt1p-mediated arginine methylation leads to the dysregulation of phosphate homeostasis. Although the monomethylation of Pho4p at Arg-241 may play a role in this process, this was not validated *in vivo* and thus the exact molecular mechanisms underlying dysregulation remain to be confirmed.

Acknowledgments—We thank the Ramaciotti Centre for Genomics and the Bioanalytical Mass Spectrometry Facility, both at the University of New South Wales, for technical support in gene expression analysis and proteomics, respectively. We acknowledge Erin O'Shea (Harvard University) for the gift of the Pho4p-GFP strain.

DATA AVAILABILITY

Data from SILAC experiments has been submitted to the ProteomeXchange Consortium (http://proteomecentral.proteomexchange.org) via the PRIDE partner repository (57) with the data set identifier PXD004054. MaxQuant output for SILAC experiments are available as supplemental Data S1 and S2. Annotated MS/MS spectra can be visualised by using MS-Viewer (http://msviewer.ucsf.edu/prospector/cgi-bin/msform.cgi?form=msviewer) with the search keys: 1olc8v6ekm (dataset A) and 0rgyw6hg1i (dataset B). RNA-Seq reads have been deposited in the NCBI sequence read archive (SRA) under the accession number SRP072252. Microarray data have been deposited in the NCBI Gene Expression Omibus under the accession number GSE99869 (58).

* MRW acknowledges financial support from the Australian Research Council (DP130100349 and DP170100108), the Australian Government NCRIS scheme, the New South Wales State Government RAAP scheme and the University of New South Wales. GHS acknowledges financial support from the Australian Research Council (DE150100019) and GHS and MAE acknowledge support from the University of New South Wales. SZC and DY acknowledge the support of Australian Postgraduate Awards.

[S] This article contains supplemental material. The authors declare they have no conflicts of interest.

‖ These authors contributed equally to this work.

¶ To whom correspondence should be addressed: Systems Biology Initiative, School of Biotechnology and Biomolecular Sciences, University of New South Wales, NSW 2052 Australia. Tel.: +61-2-9385-3633; E-mail: m.wilkins@unsw.edu.au.

Author contributions: S.Z.C., Y.-W.L., D.Y., S.L., J.J.H., and D.D. performed research; S.Z.C., Y.-W.L., D.Y., J.J.H., C.N.I.P., D.D., and Z.C. analyzed data; S.Z.C., Y.-W.L., D.Y., J.J.H., J.T.D., M.A.E., G.H.-S., and M.R.W. wrote the paper; J.T.D., M.A.E., G.H.-S., and M.R.W. designed research.

REFERENCES

1. Ong, S.-E., Mittler, G., and Mann, M. (2004) Identifying and quantifying *in vivo* methylation sites by heavy methyl SILAC. *Nat. Methods* **1,** 119–126
2. Gary, J. D., Lin, W.-J., Yang, M. C., Herschman, H. R., and Clarke, S. (1996) The predominant protein-arginine methyltransferase from *Saccharomyces cerevisiae. J. Biol. Chem.* **271,** 12585–12594
3. Ghaemmaghami, S., Huh, W. K., Bower, K., Howson, R. W., Belle, A., Dephoure, N., O'Shea, E. K., and Weissman, J. S. (2003) Global analysis of protein expression in yeast. *Nature* **425,** 737–741
4. Low, J. K. K., Hart-Smith, G., Erce, M. A., and Wilkins, M. R. (2013) Analysis of the proteome of *Saccharomyces cerevisiae* for methylarginine. *J. Proteome Res.* **12,** 3884–3899
5. Yagoub, D., Hart-Smith, G., Moecking, J., Erce, M. A., and Wilkins, M. R. (2015) Yeast proteins Gar1p, Nop1p, Npl3p, Nsr1p, and Rps2p are natively methylated and are substrates of the arginine methyltransferase Hmt1p. *Proteomics* **15,** 3209–3218
6. Hart-Smith, G., Yagoub, D., Tay, A. P., Pickford, R., and Wilkins, M. R. (2016) Large scale mass spectrometry-based identifications of enzyme-mediated protein methylation are subject to high false discovery rates. *Mol. Cell. Proteomics* **15,** 989–1006
7. Plank, M., Fischer, R., Geoghegan, V., Charles, P. D., Konietzny, R., Acuto, O., Pears, C., Schofield, C. J., and Kessler, B. M. (2015) Expanding the yeast protein arginine methylome. *Proteomics* **15,** 3232–3243
8. Kuo, M. H., Xu, X. J., Bolck, H. A., and Guo, D. (2009) Functional connection between histone acetyltransferase Gcn5p and methyltransferase Hmt1p. *Biochim. Biophys. Acta* **1789,** 395–402
9. Lacoste, N., Utley, R. T., Hunter, J. M., Poirier, G. G., and Côté, J. (2002) Disruptor of telomeric silencing-1 is a chromatin-specific histone H3 methyltransferase. *J. Biol. Chem.* **277,** 30421–30424
10. Low, J. K. K., and Wilkins, M. R. (2012) Protein arginine methylation in *Saccharomyces cerevisiae. FEBS J.* **279,** 4423–4443
11. Low, J. K., Im, H., Erce, M. A., Hart-Smith, G., Snyder, M. P., and Wilkins, M. R. (2016) Protein substrates of the arginine methyltransferase Hmt1 identified by proteome arrays. *Proteomics* **16,** 465–476
12. Zhang, X., and Cheng, X. (2003) Structure of the predominant protein arginine methyltransferase PRMT1 and analysis of its binding to substrate peptides. *Structure* **11,** 509–520
13. Yu, Z., Chen, T., Hébert, J., Li, E., and Richard, S. (2009) A mouse PRMT1 null allele defines an essential role for arginine methylation in genome maintenance and cell proliferation. *Mol. Cell Biochem.* **29,** 2982–2996
14. Wei, H., Mundade, R., Lange, K., and Lu, T. (2014) Protein arginine methylation of non-histone proteins and its role in diseases. *Cell Cycle* **13,** 32–41
15. Pawlak, M. R., Scherer, C. A., Chen, J., Roshon, M. J., and Ruley, H. E. (2000) Arginine N-methyltransferase 1 is required for early postimplantation mouse development, but cells deficient in the enzyme are viable. *Mol. Cell. Biol.* **20,** 4859–4869
16. Yu, M. C., Bachand, F., McBride, A. E., Komili, S., Casolari, J. M., and Silver, P. A. (2004) Arginine methyltransferase affects interactions and recruitment of mRNA processing and export factors. *Genes Dev.* **18,** 2024–2035
17. Yu, M. C., Lamming, D. W., Eskin, J. A., Sinclair, D. A., and Silver, P. A. (2006) The role of protein arginine methylation in the formation of silent chromatin. *Genes Dev.* **20,** 3249–3254
18. Milliman, E. J., Hu, Z., and Yu, M. C. (2012) Genomic insights of protein arginine methyltransferase Hmt1 binding reveals novel regulatory functions. *BMC Genomics* **13,** 728–728
19. Ogawa, N., DeRisi, J., and Brown, P. O. (2000) New components of a system for phosphate accumulation and polyphosphate metabolism in *Saccharomyces cerevisiae* revealed by genomic expression analysis. *Mol. Biol. Cell* **11,** 4309–4321
20. Wykoff, D. D., and O'Shea, E. K. (2001) Phosphate transport and sensing in *Saccharomyces cerevisiae. Genetics* **159,** 1491–1499
21. Hothorn, M., Neumann, H., Lenherr, E. D., Wehner, M., Rybin, V., Hassa, P. O., Uttenweiler, A., Reinhardt, M., Schmidt, A., Seiler, J., Ladurner, A. G., Herrmann, C., Scheffzek, K., and Mayer, A. (2009) Catalytic core of a membrane-associated eukaryotic polyphosphate polymerase. *Science* **324,** 513–516
22. Desfougeres, Y., Gerasimaite, R. U., Jessen, H. J., and Mayer, A. (2016) Vtc5, a novel subunit of the vacuolar transporter chaperone complex, regulates polyphosphate synthesis and phosphate homeostasis in yeast. *J. Biol. Chem.* **291,** 22262–22275
23. Thomas, M. R., and O'Shea, E. K. (2005) An intracellular phosphate buffer filters transient fluctuations in extracellular phosphate levels. *Proc. Natl. Acad. Sci. U.S.A.* **102,** 9565–9570
24. Moreno, S. N. J., and Docampo, R. (2013) Polyphosphate and its diverse functions in host cells and pathogens. *PLOS Pathog.* **9,** e1003230
25. Kornberg, A., Rao, N. N., and Ault-Riché, D. (1999) Inorganic polyphosphate: a molecule of many functions. *Annu. Rev. Biochem.* **68,** 89–125
26. Bru, S., Martinez-Lainez, J. M., Hernandez-Ortega, S., Quandt, E., Torres-Torronteras, J., Marti, R., Canadell, D., Arino, J., Sharma, S., Jimenez, J., and Clotet, J. (2016) Polyphosphate is involved in cell cycle progression and genomic stability in *Saccharomyces cerevisiae. Mol. Microbiol.* **101,** 367–380
27. Zhang, L., Hamey, J. J., Hart-Smith, G., Erce, M. A., and Wilkins, M. R. (2014) Elongation factor methyltransferase 3–a novel eukaryotic lysine methyltransferase. *Biochem. Biophys. Res. Commun.* **451,** 229–234
28. Janke, C., Magiera, M. M., Rathfelder, N., Taxis, C., Reber, S., Maekawa, H., Moreno-Borchart, A., Doenges, G., Schwob, E., Schiebel, E., and

Knop, M. (2004) A versatile toolbox for PCR-based tagging of yeast genes: new fluorescent proteins, more markers and promoter substitution cassettes. *Yeast* **21,** 947–962
29. Kaffman, A., Rank, N. M., and O'Shea, E. K. (1998) Phosphorylation regulates association of the transcription factor Pho4 with its import receptor Pse1/Kap121. *Genes Dev.* **12,** 2673–2683
30. Cox, M. P., Peterson, D. A., and Biggs, P. J. (2010) SolexaQA: At-a-glance quality assessment of Illumina second-generation sequencing data. *BMC Biochem.* **11,** 485–485
31. Engel, S. R., Dietrich, F. S., Fisk, D. G., Binkley, G., Balakrishnan, R., Costanzo, M. C., Dwight, S. S., Hitz, B. C., Karra, K., Nash, R. S., Weng, S., Wong, E. D., Lloyd, P., Skrzypek, M. S., Miyasato, S. R., Simison, M., and Cherry, J. M. (2014) The reference genome sequence of *Saccharomyces cerevisiae*: then and now. *G3* **4,** 389–398
32. Trapnell, C., Roberts, A., Goff, L., Pertea, G., Kim, D., Kelley, D. R., Pimentel, H., Salzberg, S. L., Rinn, J. L., and Pachter, L. (2012) Differential gene and transcript expression analysis of RNA-seq experiments with TopHat and Cufflinks. *Nat. Protoc.* **7,** 562–578
33. Langmead, B., Trapnell, C., Pop, M., and Salzberg, S. L. (2009) Ultrafast and memory-efficient alignment of short DNA sequences to the human genome. *Genome Biol.* **10,** R25–R25
34. Anders, S., Pyl, P. T., and Huber, W. (2014) HTSeq-a Python framework to work with high-throughput sequencing data. *Bioinformatics* 002824–002824
35. Cherry, J. M., Hong, E. L., Amundsen, C., Balakrishnan, R., Binkley, G., Chan, E. T., Christie, K. R., Costanzo, M. C., Dwight, S. S., Engel, S. R., Fisk, D. G., Hirschman, J. E., Hitz, B. C., Karra, K., Krieger, C. J., Miyasato, S. R., Nash, R. S., Park, J., Skrzypek, M. S., Simison, M., Weng, S., and Wong, E. D. (2012) Saccharomyces Genome Database: The genomics resource of budding yeast. *Nucleic Acids Res.* **40**
36. Anders, S., and Huber, W. (2010) Differential expression analysis for sequence count data. *Genome Biol.* **11,** R106–R106
37. Gentleman, R. C., Carey, V. J., Bates, D. M., Bolstad, B., Dettling, M., Dudoit, S., Ellis, B., Gautier, L., Ge, Y., Gentry, J., Hornik, K., Hothorn, T., Huber, W., Iacus, S., Irizarry, R., Leisch, F., Li, C., Maechler, M., Rossini, A. J., Sawitzki, G., Smith, C., Smyth, G., Tierney, L., Yang, J. Y. H., and Zhang, J. (2004) Bioconductor: open software development for computational biology and bioinformatics. *Genome Biol.* **5,** R80–R80
38. Gautier, L., Cope, L., Bolstad, B. M., and Irizarry, R. A. (2004) affy–analysis of Affymetrix GeneChip data at the probe level. *Bioinformatics* **20,** 307–315
39. Gillespie, C. S., Lei, G., Boys, R. J., Greenall, A., and Wilkinson, D. J. (2010) Analysing time course microarray data using Bioconductor: a case study using yeast2 Affymetrix arrays. *BMC Research Notes* **3,** 81
40. Irizarry, R. A., Hobbs, B., Collin, F., Beazer-Barclay, Y. D., Antonellis, K. J., Scherf, U., and Speed, T. P. (2003) Exploration, normalization, and summaries of high density oligonucleotide array probe level data. *Biostatistics* **4,** 249–264
41. Ritchie, M. E., Phipson, B., Wu, D., Hu, Y., Law, C. W., Shi, W., and Smyth, G. K. (2015) limma powers differential expression analyses for RNA-sequencing and microarray studies. *Nucleic Acids Res.* **43,** e47
42. Gagnon-Bartsch, J. A., Jacob, L., and Speed, T. P. (2013) Removing unwanted variation from high dimensional data with negative controls. *Technical Reports from the Department of Statistics, University of California, Berkeley*, 1–112
43. Yagoub, D., Tay, A. P., Chen, Z., Hamey, J. J., Cai, C., Chia, S. Z., Hart-Smith, G., and Wilkins, M. R. (2015) Proteogenomic discovery of a small, novel protein in yeast reveals a strategy for the detection of unannotated short open reading frames. *J. Proteome Res.* **14,** 5038–5047
44. Shevchenko, A., Tomas, H., Havlis, J., Olsen, J. V., and Mann, M. (2006) In-gel digestion for mass spectrometric characterization of proteins and proteomes. *Nat. Protoc.* **1,** 2856–2860
45. Cox, J., and Mann, M. (2008) MaxQuant enables high peptide identification rates, individualized p.p.b.-range mass accuracies and proteome-wide protein quantification. *Nat. Biotechnol.* **26,** 1367–1372
46. Consortium, U. (2015) UniProt: a hub for protein information. *Nucleic Acids Res.* **43,** D204–D212
47. Zeeberg, B. R., Feng, W., Wang, G., Wang, M. D., Fojo, A. T., Sunshine, M., Narasimhan, S., Kane, D. W., Reinhold, W. C., Lababidi, S., Bussey, K. J., Riss, J., Barrett, J. C., and Weinstein, J. N. (2003) GoMiner: a resource for biological interpretation of genomic and proteomic data. *Genome Biol.* **4,** R28–R28
48. Lev, S., Crossett, B., Cha, S. Y., Desmarini, D., Li, C., Chayakulkeeree, M., Wilson, C. F., Williamson, P. R., Sorrell, T. C., and Djordjevic, J. T. (2014) Identification of Aph1, a phosphate-regulated, secreted, and vacuolar acid phosphatase in *Cryptococcus neoformans. mBio* **5,** e01649-01614
49. Orkwis, B. R., Davies, D. L., Kerwin, C. L., Sanglard, D., and Wykoff, D. D. (2010) Novel acid phosphatase in Candida glabrata suggests selective pressure and niche specialization in the phosphate signal transduction pathway. *Genetics* **186,** 885–895
50. Canadell, D., Bru, S., Clotet, J., and Ariño, J. (2016) Extraction and quantification of polyphosphate in the budding yeast *Saccharomyces cerevisiae. Bio. Protoc.* **6,** e1874
51. Erce Ma., Low, J. K. K., Hart-Smith, G., and Wilkins, M. R. (2013) A conditional two-hybrid (C2H) system for the detection of protein-protein interactions that are mediated by post-translational modification. *Proteomics* **13,** 1059–1064
52. Erce Ma., Abeygunawardena, D., Low, J. K. K., Hart-Smith, G., and Wilkins, M. R. (2013) Interactions affected by arginine methylation in the yeast protein-protein interaction network. *Mol. Cell. Proteomics* **12,** 3184–3198
53. Hart-Smith, G., Low, J. K. K., Erce, M. A., and Wilkins, M. R. (2012) Enhanced methylarginine characterization by post-translational modification-specific targeted data acquisition and electron-transfer dissociation mass spectrometry. *J. Am. Soc. Mass Spectrom* **23,** 1376–1389
54. Winter, D. L., Hart-Smith, G., and Wilkins, M. R. (2018) Characterization of protein methyltransferases Rkm1, Rkm4, Efm4, Efm7, Set5 and Hmt1 reveals extensive post-translational modification. *J. Mol. Biol.* **430,** 102–118
55. Chiu, J., Tillett, D., Dawes, I. W., and March, P. E. (2008) Site-directed, Ligase-Independent Mutagenesis (SLIM) for highly efficient mutagenesis of plasmids greater than 8kb. *J. Microbiol. Methods* **73,** 195–198
56. Daniel Gietz, R., and Woods, R. A. (2002) Transformation of yeast by lithium acetate/single-stranded carrier DNA/polyethylene glycol method. In: Christine, G., and Gerald, R. F., eds., pp. 87–96, Academic Press
57. Vizcaíno, J. A., Csordas, A., Del-Toro, N., Dianes, J. A., Griss, J., Lavidas, I., Mayer, G., Perez-Riverol, Y., Reisinger, F., Ternent, T., Xu, Q.-W., Wang, R., and Hermjakob, H. (2016) 2016 update of the PRIDE database and its related tools. *Nucleic Acids Res.* **44,** D447–D456
58. Edgar, R., Domrachev, M., and Lash, A. E. (2002) Gene Expression Omnibus: NCBI gene expression and hybridization array data repository. *Nucleic Acids Res.* **30,** 207–210
59. Bun-Ya, M., Nishimura, M., Harashima, S., and Oshima, Y. (1991) The PHO84 gene of *Saccharomyces cerevisiae* encodes an inorganic phosphate transporter. *Mol. Cell. Proteomics* **11,** 3229–3238
60. Toh-e, A, Ueda Y, Kakimoto, S-I, and Oshima, Y. (1973) Isolation and characterization of acid phosphatase mutants in *Saccharomyces cerevisiae. J. Bacteriol.* **113,** 727–738
61. Teixeira, M. C., Monteiro, P. T., Guerreiro, J. F., Gonçalves, J. P., Mira, N. P., dos Santos, S. C., Cabrito, T. R., Palma, M., Costa, C., Francisco, A. P., Madeira, S. C., Oliveira, A. L., Freitas, A. T., and Sá-Correia, I. (2014) The YEASTRACT database: an upgraded information system for the analysis of gene and genomic transcription regulation in *Saccharomyces cerevisiae. Nucleic Acids Res.* **42,** D161–D166
62. de Godoy, L. M. F., Olsen, J. V., De Souza, G. A., Li, G., Mortensen, P., and Mann, M. (2006) Status of complete proteome analysis by mass spectrometry: SILAC labeled yeast as a model system. *Genome Biol.* **7,** R50–R50
63. Ong, S. E., Blagoev, B., Kratchmarova, I., Kristensen, D. B., Steen, H., Pandey, A., and Mann, M. (2002) Stable isotope labeling by amino acids in cell culture, SILAC, as a simple and accurate approach to expression proteomics. *Mol. Cell. Proteomics* **1,** 376–386
64. Maier, T., Guell, M., and Serrano, L. (2009) Correlation of mRNA and protein in complex biological samples. *FEBS Lett.* **583,** 3966–3973
65. Blinnikova, E. I., Mirjuschenko, F. L., Shabalin, Y. A., and Egorov, S. N. (2002) Vesicular transport of extracellular acid phosphatases in yeast *Saccharomyces cerevisiae. Biochemistry* **67,** 485–490
66. Toh-e, A, Nakamura Hand Oshima, Y. (1976) A gene controlling the synthesis of non specific alkaline phosphatase in *Saccharomyces cerevisiae. Biohim. Biophys. Acta* **428,** 182–192

67. Phelps, A., Schobert, C. T., and Wohlrab, H. (1991) Cloning and characterization of the mitochondrial phosphate transport protein gene from the yeast *Saccharomyces cerevisiae. Biochemistry* **30,** 248–252
68. Secco, D., Wang, C., Shou, H., and Whelan, J. (2012) Phosphate homeostasis in the yeast *Saccharomyces cerevisiae*, the key role of the SPX domain-containing proteins. *FEBS Lett.* **586,** 289–295
69. Cohen, A., Perzov, N., Nelson, H., and Nelson, N. (1999) A novel family of yeast chaperons involved in the distribution of V-ATPase and other membrane proteins. *J. Biol. Chem.* **274,** 26885–26893
70. Müller, O., Neumann, H., Bayer, M. J., and Mayer, A. (2003) Role of the Vtc proteins in V-ATPase stability and membrane trafficking. *J. Cell Sci.* **116,** 1107–1115
71. Uttenweiler, A., Schwarz, H., Neumann, H., and Mayer, A. (2007) The vacuolar transporter chaperone (VTC) complex is required for microautophagy. *Mol. Biol. Cell* **18,** 166–175
72. Hegelund, J. N., Jahn, T. P., Baekgaard, L., Palmgren, M. G., and Schjoerring, J. K. (2010) Transmembrane nine proteins in yeast and *Arabidopsis* affect cellular metal contents without changing vacuolar morphology. *Physiol. Plant* **140,** 355–367
73. Klionsky, D. J., and Emr, S. D. (1989) Membrane protein sorting: biosynthesis, transport and processing of yeast vacuolar alkaline phosphatase. *EMBO J.* **8,** 2241–2250
74. Xu, C., Henry, P. A., Setya, A., and Henry, M. F. (2003) In vivo analysis of nucleolar proteins modified by the yeast arginine methyltransferase Hmt1/Rmt1p. *RNA* **9,** 746–759
75. Frankel, A., and Clarke, S. (1999) RNase treatment of yeast and mammalian cell extracts affects *in vitro* substrate methylation by type I protein arginine N-methyltransferases. *Biochem. Biophys. Res. Commun.* **259,** 391–400
76. Chen, Y. C. Y.-C., Milliman, E. J., Goulet, I., Côté, J., Jackson Ca. Vollbracht Ja Yu, M. C., and Cote, J. (2010) Protein arginine methylation facilitates cotranscriptional recruitment of pre-mRNA splicing factors. *Mol. Cell. Proteomics* **30,** 5245–5256
77. Jensen, L. J., Kuhn, M., Stark, M., Chaffron, S., Creevey, C., Muller, J., Doerks, T., Julien, P., Roth, A., Simonovic, M., Bork, P., and von Mering, C. (2009) STRING 8 – A global view on proteins and their functional interactions in 630 organisms. *Nucleic Acids Res.* **37**
78. Batisse, J., Batisse, C., Budd, A., Böttcher, B., and Hurt, E. (2009) Purification of nuclear poly(A)-binding protein Nab2 reveals association with the yeast transcriptome and a messenger ribonucleoprotein core structure. *J. Biol. Chem.* **284,** 34911–34917
79. Mitchell, S. F., Jain, S., She, M., and Parker, R. (2013) Global analysis of yeast mRNPs. *Nat. Struct. Mol. Biol.* **20,** 127–133
80. Deleted in proof.
81. Srikumar, T., Lewicki, M. C., and Raught, B. (2013) A global *S. cerevisiae* small ubiquitin-related modifier (SUMO) system interactome. *Mol. Syst. Biol.* **9,** 668–668
82. Hasegawa, Y., Irie, K., and Gerber, A. P. (2008) Distinct roles for Khd1p in the localization and expression of bud-localized mRNAs in yeast. *RNA* **14,** 2333–2347
83. Ostareck-Lederer, A., Ostareck, D. H., Rucknagel, K. P., Schierhorn, A., Moritz, B., Huttelmaier, S., Flach, N., Handoko, L., and Wahle, E. (2006) Asymmetric arginine dimethylation of heterogeneous nuclear ribonucleoprotein K by protein-arginine methyltransferase 1 inhibits its interaction with c-Src. *J. Biol. Chem.* **281,** 11115–11125
84. Ghillebert, R., Swinnen, E., De Snijder, P., Smets, B., and Winderickx, J. (2011) Differential roles for the low-affinity phosphate transporters Pho87 and Pho90 in Saccharomyces cerevisiae. *Biochem. J.* **434,** 243–251
85. McBride, A. E., Weiss, V. H., Kim, H. K., Hogle, J. M., and Silver, P. A. (2000) Analysis of the yeast arginine methyltransferase Hmt1p/Rmt1p and its *in vivo* function. *J. Biol. Chem.* **275,** 3128–3136
86. Weimberg, R., and Orton, W. L. (1965) Synthesis and breakdown of the polyphosphate fraction and acid phosphomonoesterase of *Saccharomyces mellis* and their locations in the cell. *J. Bacteriol.* **89,** 740–747
87. Weimberg, R. (1975) Polyphosphate levels in nongrowing cells of *Saccharomyces mellis* as determined by magnesium ion and the phenomenon of "Uberkompensation". *J. Bacteriol.* **121,** 1122–1130
88. Shen, E. C., Henry, M. F., Weiss, V. H., Valentini, S. R., Silver, P. A., and Lee, M. S. (1998) Arginine methylation facilitates the nuclear export of hnRNP proteins. *Genes Dev.* **12,** 679–691
89. Green, D. M., Marfatia Ka Crafton, E. B., Zhang, X., Cheng, X., and Corbett, A. H. (2002) Nab2p is required for poly(A) RNA export in *Saccharomyces cerevisiae* and is regulated by arginine methylation via Hmt1p. *J. Biol. Chem.* **277,** 7752–7760
90. Henry, M. F., and Silver, P. A. (1996) A novel methyltransferase (Hmt1p) modifies poly(A)+-RNA-binding proteins. *Mol. Cell. Proteomics* **16,** 3668–3678
91. Magbanua, J. P., Ogawa, N., Harashima, S., and Oshima, Y. (1997) The transcriptional activators of the PHO regulon, Pho4p and Pho2p, interact directly with each other and with components of the basal transcription machinery in *Saccharomyces cerevisiae. J. Biol. Chem.* **121,** 1182–1189
92. O'Neill, E. M., Kaffman, A., Jolly, E. R., and O'Shea, E. K. (1996) Regulation of PHO4 nuclear localization by the PHO80-PHO85 cyclin-CDK complex. *Science* **271,** 209–212
93. Komeili, A., and O'Shea, E. K. (1999) Roles of phosphorylation sites in regulating activity of the transcription factor Pho4. *Science* **284,** 977–980
94. Mutvei, A., Dihlmann, S., Herth, W., and Hurt, E. C. (1992) NSP1 depletion in yeast affects nuclear pore formation and nuclear accumulation. *Eur J. Cell Biol.* **59,** 280–295
95. Xu, C., and Henry, M. F. (2004) Nuclear export of hnRNP Hrp1p and nuclear export of hnRNP Npl3p are linked and influenced by the methylation state of Npl3p. *Mol. Cell. Biol.* **24,** 10742–10756
96. Huh, W.-K., Falvo, J. V., Gerke, L. C., Carroll, A. S., Howson, R. W., Weissman, J. S., and O'Shea, E. K. (2003) Global analysis of protein localization in budding yeast. *Nature* **425,** 686–691
97. Leggett, J. E., and Olsen, R. A. (1964) Anion absorption by baker's yeast. *Plant Physiol.* **39,** 387–390
98. Müller, O., Bayer, M. J., Peters, C., Andersen, J. S., Mann, M., and Mayer, A. (2002) The Vtc proteins in vacuole fusion: coupling NSF activity to V(0) trans-complex formation. *EMBO J.* **21,** 259–269
99. Azevedo, C., Livermore, T., and Saiardi, A. (2015) Protein polyphosphorylation of lysine residues by inorganic polyphosphate. *Mol. Cell* **58,** 71–82
100. Windgassen, M., Sturm, D., Cajigas, I. J., González, C. I., Seedorf, M., Bastians, H., and Krebber, H. (2004) Yeast shuttling SR proteins Npl3p, Gbp2p, and Hrb1p are part of the translating mRNPs, and Npl3p can function as a translational repressor. *Mol. Cell. Biol.* **24,** 10479–10491
101. Kaffman, A., Rank, N. M., O'Neill, E. M., Huang, L. S., and O'Shea, E. K. (1998) The receptor Msn5 exports the phosphorylated transcription factor Pho4 out of the nucleus. *Nature* **396,** 482–482
102. Shao, D., Creasy, C. L., and Bergman, L. W. (1998) A cysteine residue in helixII of the bHLH domain is essential for homodimerization of the yeast transcription factor Pho4p. *Nucleic Acids Res.* **26,** 710–714
103. Shimizu, T., Toumoto, A., Ihara, K., Shimizu, M., Kyogoku, Y., Ogawa, N., Oshima, Y., and Hakoshima, T. (1997) Crystal structure of PHO4 bHLH domain-DNA complex: Flanking base recognition. *EMBO J.* **16,** 4689–4697
104. McBride, A. E., Cook, J. T., Stemmler Ea Rutledge, K. L., McGrath Ka., Rubens, J. a (2005) . Arginine methylation of yeast mRNA-binding protein Npl3 directly affects its function, nuclear export, and intranuclear protein interactions. *J. Biol. Chem.* **280,** 30888–30898
105. Baierlein, C., Hackmann, A., Gross, T., Henker, L., Hinz, F., and Krebber, H. (2013) Monosome formation during translation initiation requires the serine/arginine-rich protein Npl3. *Mol. Cell. Proteomics* **33,** 4811–4823
106. Winter, D. L., Erce, M. A., and Wilkins, M. R. (2014) A web of possibilities: network-based discovery of protein interaction codes. *J. Proteome Res.* **13,** 5333–5338
107. Albuquerque, C. P., Smolka, M. B., Payne, S. H., Bafna, V., Eng, J., and Zhou, H. (2008) A multidimensional chromatography technology for in-depth phosphoproteome analysis. *Mol. Cell. Proteomics* **7,** 1389–1396
108. Chi, A., Huttenhower, C., Geer, L. Y., Coon, J. J., Syka, J. E. P., Bai, D. L., Shabanowitz, J., Burke, D. J., Troyanskaya, O. G., and Hunt, D. F. (2007) Analysis of phosphorylation sites on proteins from *Saccharomyces cerevisiae* by electron transfer dissociation (ETD) mass spectrometry. *Proc. Natl. Acad. Sci. U.S.A.* **104,** 2193–2198
109. Zappacosta, F., Collingwood, T. S., Huddleston, M. J., and Annan, R. S. (2006) A quantitative results-driven approach to analyzing multisite

protein phosphorylation: the phosphate-dependent phosphorylation profile of the transcription factor Pho4. *Mol. Cell. Proteomics* **5,** 2019–2030

110. Chen, W., Daines, M. O., and Hershey, G. K. K. (2004) Methylation of STAT6 modulates STAT6 phosphorylation, nuclear translocation, and DNA-binding activity. *J. Immunol.* **172,** 6744–6750
111. Yang, J.-H., Chiou, Y.-Y., Fu, S.-L., Shih, I. Y., Weng, T.-H., Lin, W.-J., and Lin, C.-H. (2014) Arginine methylation of hnRNPK negatively modulates apoptosis upon DNA damage through local regulation of phosphorylation. *Nucleic Acids Res.* **42,** 9908–9924
112. Hardiville, S., and Hart, G. W. (2014) Nutrient regulation of signaling, transcription, and cell physiology by O-GlcNAcylation. *Cell Metabolism* **20,** 208–213
113. Kanai, M., Masuda, M., Takaoka, Y., Ikeda, H., Masaki, K., Fujii, T., and Iefuji, H. (2013) Adenosine kinase-deficient mutant of *Saccharomyces cerevisiae* accumulates S-adenosylmethionine because of an enhanced methionine biosynthesis pathway. *Appl. Microbiol. Biotechnol.* **97,** 1183–1190
114. Albaugh, B. N., Arnold, K. M., and Denu, J. M. (2011) KAT(ching) Metabolism by the Tail: Insight into the links between lysine acetyltransferases and metabolism. *ChemBioChem.* **12,** 290–298